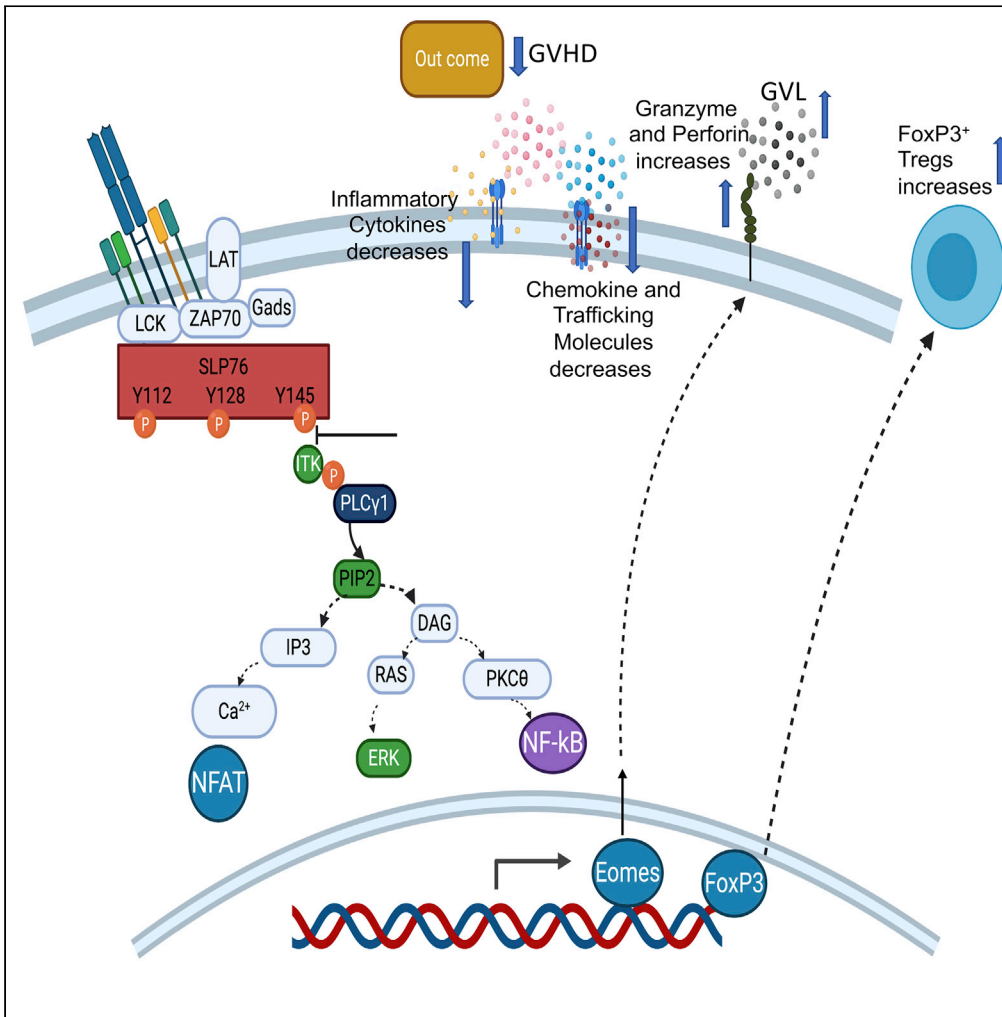


Article

Targeting SLP76:ITK interaction separates GVHD from GVL in allo-HSCT



For a Figure360 author presentation of this figure, see <https://doi.org/10.1016/j.isci.2021.102286>.

Mahinbanu Mammadli, Weishan Huang, Rebecca Harris, ..., Avery August, Alaji Bah, Mobin Karimi

karimim@upstate.edu

Highlights

SLP76Y145FKI donor T cells exhibit minimal GVHD but maintain GVL activity

Inhibiting SLP76:ITK signaling by a novel peptide reduces GVHD while retaining GVL



Article

Targeting SLP76:ITK interaction separates GVHD from GVL in allo-HSCT

Mahinbanu Mammadli,¹ Weishan Huang,^{2,4} Rebecca Harris,¹ Hui Xiong,⁵ Samuel Weeks,¹ Adriana May,¹ Teresa Gentile,³ Jessica Henty-Ridilla,⁶ Adam T. Waickman,¹ Avery August,⁴ Alaji Bah,⁶ and Mobin Karimi^{1,7,*}

SUMMARY

Allogeneic hematopoietic stem cell transplantation (allo-HSCT) is a curative therapy for hematological malignancies, due to graft-versus-leukemia (GVL) activity mediated by alloreactive donor T cells. However, graft-versus-host disease (GVHD) is also mediated by these cells. Here, we assessed the effect of attenuating TCR-mediated SLP76:ITK interaction in GVL vs. GVHD effects after allo-HSCT. CD8⁺ and CD4⁺ donor T cells from mice expressing a Y145F mutation in SLP-76 did not cause GVHD but preserved GVL effects against B-ALL cells. SLP76Y145FKI CD8⁺ and CD4⁺ donor T cells also showed less inflammatory cytokine production and migration to GVHD target organs. We developed a novel peptide to specifically inhibit SLP76:ITK interactions, resulting in decreased phosphorylation of PLC γ 1 and ERK, decreased cytokine production in human T cells, and separation of GVHD from GVL effects. Altogether, our data suggest that inhibiting SLP76:ITK interaction could be a therapeutic strategy to separate GVHD from GVL effects after allo-HSCT treatment.

INTRODUCTION

Graft-versus-host disease (GVHD) is primarily orchestrated by mature donor T cells (Breems and Lowenberg, 2005). Mature T cells in the graft facilitate stem cell engraftment and, most importantly, ensure the therapeutic graft-versus-leukemia (GVL) effect (Breems and Lowenberg, 2005; Tugues et al., 2018). However, these alloreactive T cells also facilitate the unwanted effect of GVHD (Bastien et al., 2012). Standard immunosuppressive therapy for GVHD is not optimal because it leaves patients susceptible to opportunistic infections such as Cytomegalovirus and relapse of the malignancy being treated (Bleakley et al., 2012) (Ferrara, 2014). The pathophysiology of GVHD depends upon interactions between donor T cells and host antigen-presenting cells (APCs). T cell receptor (TCR)-mediated activation of donor T cells by APCs is critical for both GVHD and GVL effects (Guinan et al., 1999). Following TCR activation and expansion in secondary lymphoid organs, the alloreactive T cells migrate to target organs and cause tissue damage by producing inflammatory cytokines and by exhibiting cytotoxicity against healthy tissues (Ferrara, 2014). Thus, GVHD can be treated by interfering with T cell activation and proliferation using calcineurin inhibitors (cyclosporine, tacrolimus), mTOR inhibitors (sirolimus), and antiproliferative agents (methotrexate, cyclophosphamide, or mycophenolate) (Reddy and Ferrara, 2008; Baxter and Hodgkin, 2002). However, while alleviating GVHD, global inhibition of T cell activation also negates the beneficial GVL effect. Thus, specific signaling pathways, which can be targeted to allow GVL effects to occur while inhibiting GVHD, need to be identified. T cell signaling requires a multimolecular proximal signaling complex, which consists of adapter proteins such as SLP76 (Koretzky et al., 2006; Kambayashi et al., 2009). SLP is involved in phosphorylation of phospholipase C-gamma isoforms by IL-2-inducible T cell kinase (ITK) in T cells (Su et al., 1999). ITK is a critical mediator of TCR signaling (Bunnell et al., 2000).

SLP-76 activates ITK through its N-terminal tyrosine at the position Y145 (Bogin et al., 2007; Jordan et al., 2006). When phosphorylated, the tyrosine residue 145 (Y145) of SLP76 binds to and activates the Tec family tyrosine kinase ITK (Bogin et al., 2007). Thus, a Y→F mutation at Y145 of SLP76 leads to defective TCR-mediated ITK activation (Jordan et al., 2006). The SLP76 Y145 and ITK interaction is involved in signaling pathways that lead to cytokine production by T cell populations, as well as in regulating the development of a distinct, innate-type cytokine-producing T cell population in the thymus (Atherly et al., 2006), referred to as innate memory phenotype (IMP) T cells. CD4⁺ and CD8⁺ T cells from SLP76Y145FKI mice express significantly higher CD122, CD44, and Eomes compared to T cells from WT mice on a basal, unstimulated

¹Department of Microbiology and Immunology, SUNY Upstate Medical University, 766 Irving Avenue, Weiskotten Hall Suite 2281, Syracuse, NY 13210, USA

²Department of Pathobiological Sciences, School of Veterinary Medicine, Louisiana State University, Baton Rouge, LA 70803, USA

³Division of Hematology, translational research, SUNY Upstate Medical University, Syracuse NY 13210, USA

⁴Department of Microbiology and Immunology, College of Veterinary Medicine, Cornell University, Ithaca, NY 14853, USA

⁵Department of Radiology, Jiangxi Health Vocational College, Nanchang, 330052, China

⁶Department of Biochemistry and Molecular Biology, SUNY Upstate Medical University, Syracuse, NY 13210, USA

⁷Lead contact

*Correspondence: karimim@upstate.edu

<https://doi.org/10.1016/j.isci.2021.102286>



level (Mammadli et al., 2020). Since the activation, expansion, cytokine production, and migration of alloreactive donor T cells to target organs are hallmarks of GVHD (Henden and Hill, 2015; Lynch Kelly et al., 2015), efforts to understand signaling pathways that allow separation from GVL will enable us to develop target-specific therapeutic modulators. Both CD4⁺ and CD8⁺ T cells with CD44 low (CD44^{lo}) are considered naive cells. CD4⁺ and CD8⁺ T cells with CD44 high (CD44^{hi}) are considered antigen-experienced and activated cells. Both CD4⁺ and CD8⁺ T cells from SLP76Y145F- and ITK-deficient mice express a higher proportion of cells with CD44^{hi} and CD122^{hi} (Mammadli et al., 2020). Both CD4⁺ and CD8⁺ T cells with CD44^{hi} and CD122^{hi} from SLP76Y145FKI- and ITK-deficient mice arise in the thymus during development, unlike memory CD44^{hi} CD4⁺ and CD8⁺ T cells that mainly arise in the periphery of WT mice in response to foreign antigens or because of homeostatic proliferation (Mammadli et al., 2020). Experimental studies in CD44^{hi} and CD44^{lo} cells arising in the periphery of WT mice show conflicting results (Dutt et al., 2011; Zheng et al., 2009; Loschi et al., 2015; Anderson, 2003; Huang et al., 2019). In this report, we show that WT CD8⁺CD44^{lo} T cells induce severe GVHD, and that while WT CD8⁺CD44^{hi} T cells induce less GVHD, as has been reported, they eventually cause GVHD (Zhang et al., 2005; Huang et al., 2019). In contrast, SLP76Y145FKI CD8⁺CD44^{lo} T cells are much less likely to induce GVHD, and SLP76Y145FKI CD8⁺CD44^{hi} T cells do not cause GVHD but maintain a significant GVL effect (Mammadli et al., 2020). Both CD8⁺ and CD4⁺ SLP76Y145FKI T cells exhibit attenuated TCR signaling and an IMP as indicated by expression of high levels of CD44 and CD122, and CD8⁺ SLP76Y145FKI T cells also express higher levels of the transcription factor Eomes (Huang et al., 2014; Carty et al., 2014). Our data suggest that IMP phenotype may not be enough to separate the wanted effect of GVL from the unwanted GVHD effect. We also show that disruption of the SLP76Y145/ITK interaction allows T cells to differentiate GVHD from GVL effects. Proinflammatory cytokines play a key role in the development of GVHD pathophysiology (Holler, 2002), and we further show that both CD4⁺ and CD8⁺ T cells from SLP76Y145FKI mice have reduced proinflammatory cytokine production, both on a serum level and a cellular level. Next, we examined how CD8⁺ T cells from SLP76Y145FKI mice maintained GVL effects. We also observed that about 70–80% CD8⁺ T cells from SLP76 Y145FKI and ITK-deficient mice express Eomes, and we found these Eomes-expressing cells to be critical for GVL effects. We further provided evidence that Eomes-deficient WT or SLP76Y145FKI T cells did not mount a cytotoxic response against primary leukemia cells, both *in vitro* and *in vivo* (Cheng et al., 2016). Disrupting SLP76Y145 and ITK signaling in T cells also led to defects in migration to GVHD target organs.

Finally, to make our findings clinically relevant, we developed a novel peptide inhibitor, named SLP76145pTYR, that disrupts the interaction between SLP76 and ITK (Stritesky et al., 2012). We show that SLP76145pTYR specifically inhibits the phosphorylation of ITK and downstream signaling molecules, including PLCγ1 and ERK, in both human and mouse T cells (Kim et al., 2009). Furthermore, treating T cells with SLP76pTYR enhances the development of FoxP3⁺ mouse regulatory T cells, while significantly reducing IFN-γ (Lu and Waller, 2009) and TNF-α (Mancusi et al., 2018) production by T cells from primary healthy human blood samples. Finally, SLP76145pTYR significantly reduced GVHD pathophysiology but maintained GVL function in a murine allogeneic hematopoietic stem cell transplantation (allo-HSCT) major mismatch model. Our studies therefore identify a novel, specific inhibitor capable of separating GVHD and GVL after allo-HSCT, with potential benefits for other T cell-mediated diseases as well (Summary Figure).

RESULTS

Disruption of ITK: SLP76 Y145 signaling allows tumor clearance without inducing GVHD

We recently showed that ITK is differentially required for GVHD and GVL (Mammadli et al., 2020). Therefore, we tested whether this distinction depends on the interaction of ITK with SLP76. T cell signaling requires a multimolecular proximal signaling complex that includes adapter proteins such as SLP76 (Koretzky et al., 2006; Kambayashi et al., 2009). When SLP76 is phosphorylated on tyrosine residue 145 (Y145), it binds to and activates the Tec family tyrosine kinase ITK (Bogin et al., 2007). Thus, a Y → F mutation at Y145 of SLP76 leads to defective TCR-mediated ITK activation (Jordan et al., 2006), with effects on signaling pathways that lead to cytokine production by T cell populations. Given the role of SLP76 in regulating ITK signaling downstream of the TCR, we tested whether GVL effects would remain intact when allo-BMT was performed with T cells from SLP76 Y145FKI mice. To induce GVHD, we used MHC-mismatched donors and recipients, with T cell-depleted bone marrow (T_{CD}BM) from B6.PL-Thy1a/CyJ (Thy1.1) mice, donor T cells from C57BL/6 (B6) WT or SLP76Y145FKI mice (MHC haplotype b), and lethally irradiated BALB/c (MHC haplotype d) mice as recipients. Recipient mice were injected intravenously with 10X10⁶ wild-type (WT) T_{CD}BM cells along with 2X10⁶ FACS-sorted donor T cells (1X10⁶ CD8⁺ and 1X10⁶ CD4⁺). 2X10⁵ luciferase-expressing primary B-cell acute lymphoblastic leukemia (B-ALL)-luc blast cells as previously described (Cheng et al.,

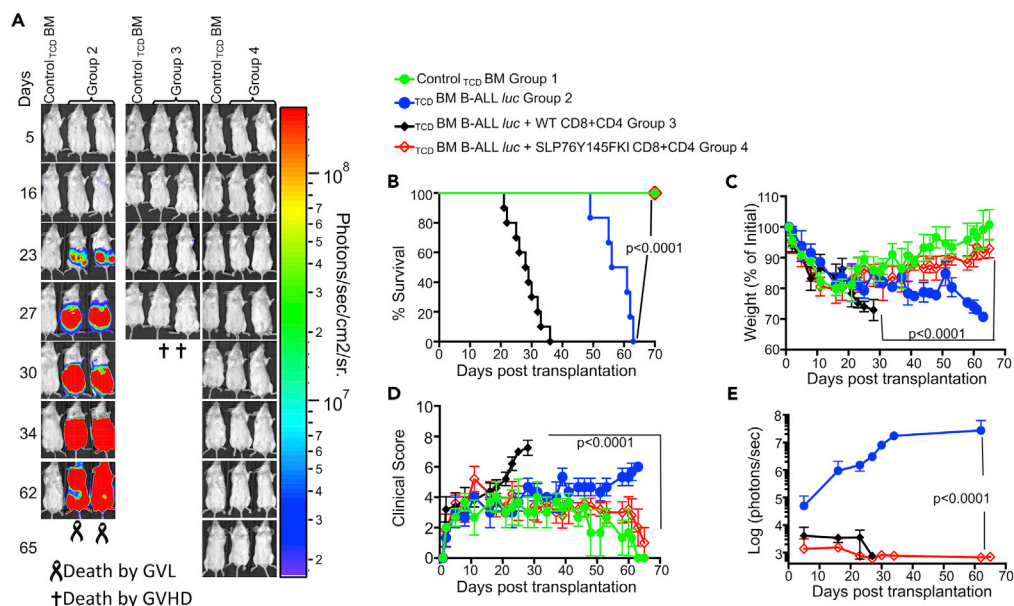


Figure 1. Disruption of ITK \rightarrow SLP76 Y145 signaling allows tumor clearance without inducing GVHD

1×10^6 purified CD8⁺ T cells and 1×10^6 purified CD4⁺ T cells from WT or SLP76 Y145FKI mice were mixed at a 1:1 ratio and transplanted with 2×10^5 B-ALL cells and 10×10^6 T cell-depleted bone marrow ($T_{CD}BM$) cells transplanted into irradiated BALB/c mice. Host BALB/c mice were imaged using the IVIS 50 system three times a week.

(A) Group one received 10×10^6 T cell depleted bone marrow cells ($T_{CD}BM$) only. Group one mice are used as negative controls while imaging other groups that have luciferase-expressing primary leukemia cells. Group two received 10×10^6 $T_{CD}BM$ with 2×10^5 B-ALL-*luc* cells ($T_{CD}BM$ + B-ALL *luc*). The third group was transplanted with 10×10^6 $T_{CD}BM$ cells and 1×10^6 purified WT CD8⁺ and 1×10^6 CD4⁺ T cells (1:1 ratio) along with 2×10^5 B-ALL-*luc* cells ($T_{CD}BM$ + B-ALL-*luc* + WT CD8⁺ and CD4⁺). Group four received 10×10^6 $T_{CD}BM$ cells and 1×10^6 purified CD8⁺ and 1×10^6 CD4⁺ T cells (1:1 ratio from SLP76 Y145FKI) along with 2×10^5 B-ALL-*luc* B-ALL-*luc* cells ($T_{CD}BM$ + B-ALL^{*luc*} + SLP76Y145F CD8+CD4).

(B–D) (B) We monitored the survival of recipient animals, (C) body weight changes, and (D) clinical score for 65 days post-BMT. For weight changes and clinical score, one representative of 2 independent experiments is shown ($n = 3$ mice/group for BM alone; $n = 5$ experimental mice/group for all three groups).

(E) We have quantitated tumor growth via luciferase bioluminescence. Statistical analysis for survival and the clinical score was performed using the log rank test and two-way ANOVA, respectively. Note: Controls are naive for cancer, but transplanted with 10×10^6 T cell depleted bone marrow alone ($T_{CD}BM$) and used as a negative control for BLI. See also Figures S1 and S2.

2016) were mixed with $T_{CD}BM$ and CD4 and CD8 T cells, and intravenously injected into recipient BALB/c mice by tail vein. B-ALL is a primary B cell acute lymphoblastic leukemia, syngeneic to BALB/c mice and allogeneic to C57BL/6 (B6) mice. B-ALL cells were mixed with donor T cells and $T_{CD}BM$ right before injection. Recipient BALB/c mice were monitored for cancer cell growth using IVIS bioluminescence imaging for over 60 days (Figure 1A). Although leukemia cell growth was observed in mice given T cell-depleted BM but no T cells, leukemia cell growth was not seen in mice transplanted with CD4⁺ and CD8⁺ T cells from either WT or SLP76Y145FKI mice. As expected, mice transplanted with WT CD4⁺ and CD8⁺ T cells suffered from GVHD, while mice transplanted with SLP76 Y145FKI CD4⁺ and CD8⁺ T cells displayed minimal signs of GVHD and survived for >65 days post-HSCT and tumor challenge (Figure 1). Most animals transplanted with SLP76Y145FKI T cells survived for more than 65 days post-allo-HSCT (Figure 1B), with significantly better survival and reduced clinical scores compared to those transplanted with WT T cells (scored based on weight, posture, activity, fur texture, and skin integrity as previously described (Cooke et al., 1996) (Figures 1C and 1D)). BALB/c mice transplanted with SLP76Y145FKI T cells showed only residual tumor cell growth (as measured by bioluminescence), indicating that the donor cells maintained GVL functions similar to WT T cells (Figure 1E). Donor CD8⁺ T cells are more potent than CD4⁺ T cells in mediating GVL effects, but both CD4⁺ and CD8⁺ T cells mediate severe GVHD in mice and humans (Amir et al., 2012; Yu et al., 2006; Wu et al., 2013). To determine whether CD4⁺ T cell-intrinsic SLP76:ITK signaling might be sufficient to induce GVHD, we repeated the same experiments using purified CD4⁺ T cells from either WT or SLP76Y145FKI mice in the MHC-mismatch mouse model of allo-HSCT (B6 \rightarrow BALB/c) (Figures S1A–S1C). Recipients of

WT CD4⁺ T cells exhibited worse survival than mice receiving $\tau_{CD}BM$ cells alone (Figure S1A). In contrast, recipients of $\tau_{CD}BM$ mixed with SLP76Y145FKI CD4⁺ T cells had greatly reduced mortality and clinical scores compared to those given WT CD4⁺ T cells (Figure S1C), indicating that CD4⁺ T cell-intrinsic SLP76:ITK signaling can contribute to the severity of GVHD.

To test whether the IMP observed in SLP76Y145FKI T cells is necessary to separate the effects of GVL from GVHD, irradiated recipient BALB/c (MHC haplotype d) mice were transplanted with sorted CD8⁺ CD44^{hi} (expressing the IMP) or CD8⁺ CD44^{lo} (control) T cells from WT or SLP76Y145FKI mice (Figure S2A). Before transplantation into recipient mice, donor T cells were examined for CD44 expression before and after sorting based on CD44 expression. Recipient mice were injected with 10X10⁶ WT C57Bl/6 $\tau_{CD}BM$ cells, with or without 1X10⁶ FACS-sorted CD8⁺ CD44^{lo} CD122^{lo} or CD8⁺ CD44^{hi} CD122^{hi} (IMP) T cells from WT or SLP76Y145FKI mice (Figure S2B). Recipient mice were challenged with 1X10⁵ primary B-ALL-*luc* (Cheng et al., 2016) tumor cells and monitored for survival, weight changes, clinical score, and tumor burden (monitored by bioluminescence imaging twice a week) for at least 60 days (Figure S2B). We found that WT CD8⁺ CD44^{lo} CD122^{lo} T cells cleared the tumor, but recipients developed acute GVHD, while WT CD8⁺ CD44^{hi} CD122^{hi} IMP T cells cleared the tumor but exhibited delayed induction of GVHD. In contrast, CD8⁺ CD44^{hi} CD122^{hi} IMP (Mammadli et al., 2020) T cells from SLP76Y145FKI mice cleared the tumor, but recipients did not develop GVHD, while CD8⁺ CD44^{lo} CD122^{lo} T cells from SLP76Y145FKI mice cleared the tumor effectively, but three out of 10 mice developed GVHD. These data indicate that WT donor CD8⁺ CD44^{hi} CD122^{hi} IMP T cells exhibited delayed GVHD but eventually caused GVHD, while SLP76Y145FKI CD8⁺ CD44^{hi} CD122^{hi} IMP T cells induce GVL but avoid the induction of GVHD (Figures S2B–S2F).

SLP76Y145FKI T cells produce less proinflammatory cytokines and exhibit reduced proliferation

Proinflammatory cytokine production by donor T cells is considered to be one of the hallmarks of GVHD (D'Aveni et al., 2015). To assess whether CD4⁺ or CD8⁺ T cells with attenuated TCR signaling produce inflammatory cytokines similar to CD4⁺ or CD8⁺ T cells from WT mice, we transplanted 1X10⁶ CD4⁺ or CD8⁺ T cells in separate experiments from either WT mice or SLP76Y145FKI mice to irradiated BALB/c mice as recipients. At day seven post-transplantation, recipient BALB/c mice were sacrificed, and serum was obtained and assessed for levels of the proinflammatory cytokines IL-33, IL-1 α , IFN- γ , TNF- α , and IL-17A by multiplex ELISA (Figures 2A and 2B). We discovered that recipient animals transplanted with CD4⁺ or CD8⁺ T cells (in separate experiments) from SLP76Y145FKI mice had significantly less production of proinflammatory cytokines compared to recipient mice transplanted with CD4⁺ or CD8⁺ T cells from WT mice (Figures 2A and 2B). To examine the sources of these observed proinflammatory cytokines, we restimulated spleen cells from recipient mice that were transplanted with CD4⁺ or CD8⁺ T cells from WT or SLP76Y145FKI mice in separate experiments. Spleen cells were restimulated with anti-CD3 and anti-CD28 in the presence of Brefeldin A, and donor CD4⁺ and CD8⁺ T cells were gated by flow cytometry using anti-H2K^b antibodies (expressed by donor cells), anti-CD3, anti-CD4, and anti-CD8. We observed that donor CD4⁺ and CD8⁺ T cells from SLP76Y145FKI mice produced significantly less IFN- γ and TNF- α compared to donor CD4⁺ and CD8⁺ T cells from WT mice. Thus, these data confirm that the changes in proinflammatory cytokine serum levels result from changes in production by the donor T cells, and that T cells from TCR-attenuated mice produce less inflammatory cytokines (Figures 2C–2E). To examine whether SLP76Y145FKI T cells are capable of producing cytokines in general, spleen cells from recipient mice transplanted with either WT or SLP76Y145FKI T cells were stimulated with PMA/ionomycin (to bypass the proximal signaling defect (Figure S3)), or left unstimulated for 6 hr in the presence of Brefeldin A, followed by the analysis of IFN- γ and TNF- α production. SLP76Y145FKI T cells were capable of producing IFN- γ and TNF- α when T cell signaling was bypassed by re-stimulation with PMA and ionomycin (Figure S3); however, compared to WT T cells, they produced significantly less inflammatory cytokines when stimulated via TCR (anti-CD3 and anti-CD28) (Figures 2C–2E). Next, we determined whether the reduction in cytokine production by SLP76Y145FKI donor T cells was due to cell-intrinsic or cell-extrinsic factors. We mixed purified SLP76Y145FKI CD8⁺ and CD4⁺ T cells with purified WT CD8⁺ or CD4⁺ T cells separately at a 1:1 ratio, and transplanted the mixed cells into irradiated BALB/c mice as described above. The congenic markers CD45.1 (WT C57BL/6) and CD45.2 (SLP76Y145FKI) were used to distinguish donor cells from the different strains of mice within the same recipient. On day 7, donor T cells were isolated from recipient mice using flow cytometry (anti-H2K^b) and examined for IFN- γ and TNF- α expression as described above. We found that WT donor CD8⁺

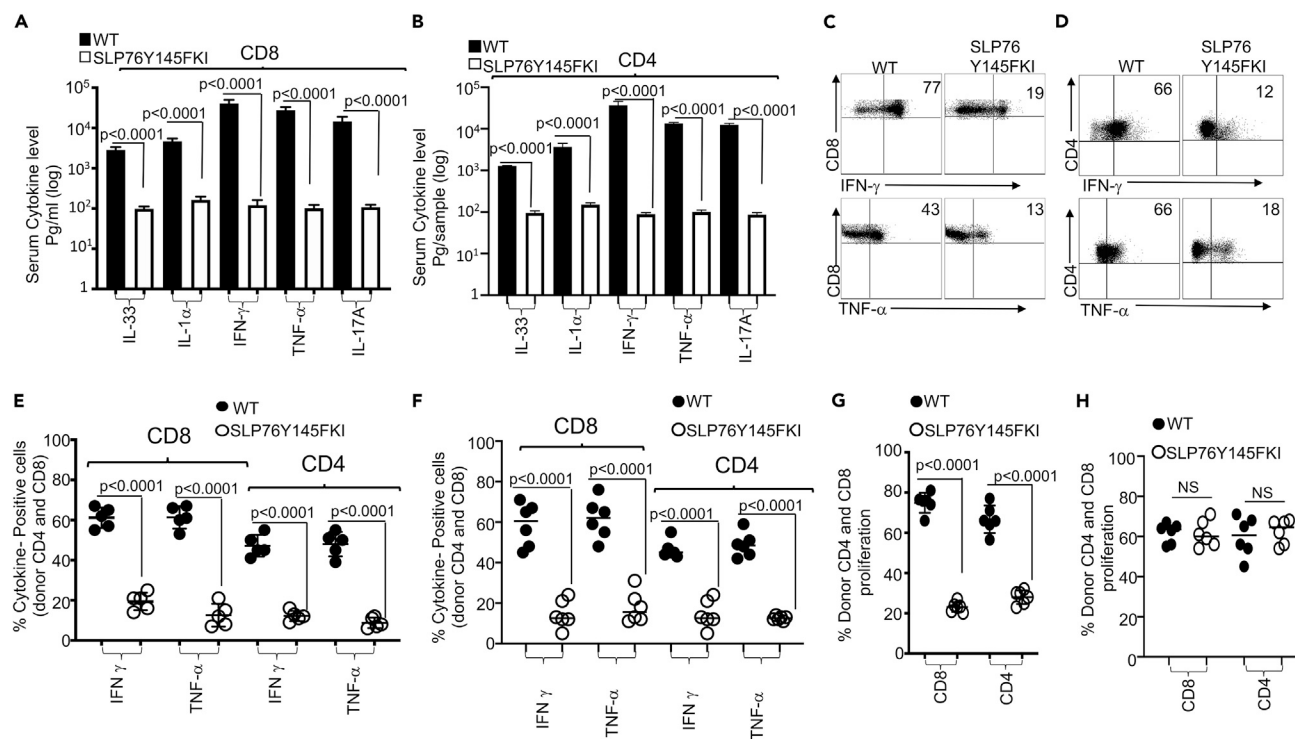


Figure 2. SLP76Y145FKI donor CD8⁺ and CD4⁺ T cells exhibit reduced cytokine production and reduced proliferation

1X10⁶ purified CD8⁺ or CD4⁺ T cells from C57Bl/6 WT or C57Bl/6 SLP76Y145FKI (MHC haplotype b) mice were transplanted into irradiated BALB/c (MHC haplotype d) mice in separate experiments.

(A and B) At day seven post-allo-HSCT, recipient BALB/c mice transplanted with either CD8⁺ or CD4⁺ T cells were euthanized, and ELISA was performed to determine serum cytokines (IL-33, IL1 α , IFN- γ , TNF- α , and IL-17A) from recipient mice.

(C and D) Donor CD4⁺ or CD8⁺ T cells were examined for IFN- γ and TNF- α by intracellular staining after stimulation with anti-CD3/anti-CD28, as determined by flow cytometry.

(E) Donor CD8⁺ or CD4⁺ T cells from several experiments were examined for IFN- γ and TNF- α as above.

(F) Flow cytometry analysis of purified CD4⁺ or CD8⁺ WT and SLP76Y145FKI T cells that were mixed at a 1:1 ratio for transplantation into irradiated BALB/c mice. At day seven donor T cells were stimulated with anti-CD3/anti-CD28 and then were gated for expression of H-2K^b, CD45.1, CD45.2. on WT T cells and SLP76Y145FKI cells and intracellular expression of IFN- γ and TNF- α analyzed by flow cytometry. Combined data from two independent experiments is shown, and the p value for each experiment is shown.

(G) Purified CD8⁺ or CD4⁺ WT or SLP76Y145FKI donor T cells were transplanted into irradiated BALB/c mice. On day seven, donor T cells were analyzed for donor CD8⁺ or CD4⁺ T cell proliferation by examining BrdU incorporation by flow cytometry.

(H) Purified CD8⁺ or CD4⁺ T cells from WT or SLP76Y145FKI mice were mixed at a 1:1 WT:SLP76Y145FKI ratio and transplanted into irradiated BALB/c mice. At day 7, splenic donor T cells were gated for the expression of H-2K^b, CD45.1, and CD45.2 and analyzed for BrdU incorporation. See also Figure S3.

and CD4⁺ T cells (CD45.1) produced higher levels of inflammatory cytokines than SLP76Y145FKI donor CD8⁺ and CD4⁺ T cells (CD45.2), suggesting that the reduced cytokine production observed by SLP76Y145FKI donor T cells is T cell-intrinsic (Figure 2F).

Next, we examined whether SLP76Y145FKI donor T cells proliferated similarly to WT donor CD4⁺ and CD8⁺ T cells. Lethally irradiated recipient BALB/c mice were transplanted as mentioned above, with either WT or SLP76Y145FKI donor CD4⁺ or CD8⁺ T cells. Recipient mice were injected with BrdU as described, and seven days post-allotransplantation, recipient mice were sacrificed and examined for proliferation by BrdU incorporation. SLP76Y145FKI donor T cells showed reduced proliferation compared to WT donor T cells Figure 2G. To determine if the reduced proliferation by SLP76Y145FKI donor T cells was due to cell-intrinsic mechanisms, we mixed sort-purified SLP76Y145FKI and WT CD4⁺ and CD8⁺ at a 1:1 ratio, followed by transplantation as described above in (Figure 2G). Interestingly, no difference was observed in BrdU incorporation by WT and SLP76Y145FKI donor CD4⁺ and CD8⁺ T cells in spleens of recipient mice in the mixed transplant models, indicating that the reduced proliferation of donor SLP76Y145FKI T cell proliferation was due to cell-extrinsic effects (Figure 2H).

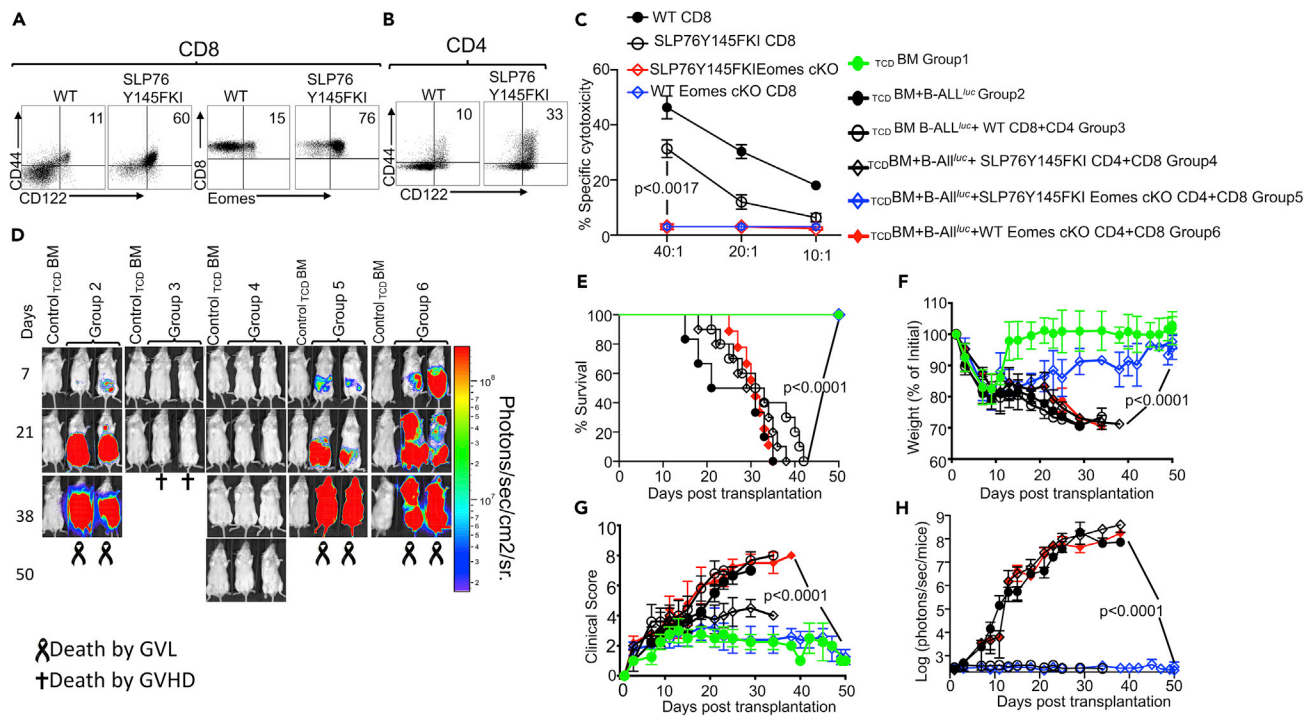


Figure 3. Eomes is required for cytotoxicity and GVL effect by both WT and SLP76Y145FKI T cells

(A and B) Purified WT and SLP76Y145FKI CD8⁺ and CD4⁺ T cells were examined for expression of CD44, CD122, and Eomes by flow cytometry. (C) Purified donor CD8⁺ T cells from either WT or SLP76 Y145FKI Eomes-sufficient, Eomes-deficient, or Eomes-flox control mice were transplanted into irradiated BALB/c (MHC haplotype d) mice. On day seven, donor T cells were purified as described and used in an ex vivo cytotoxicity assay against B-ALL-luc cells at 40:1, 20:1, and 10:1 ratios. (D) 1X10⁶ purified WT or SLP76Y145FKI Eomes-sufficient, Eomes-deficient, or Eomes-flox control CD8⁺ T cells and 1X10⁶ purified CD4⁺ T cells were mixed and transplanted along with 2X10⁵ B-ALL-luc cells and 10 × 10⁶ T cell-depleted bone marrow T_{CD}BM cells into irradiated BALB/c mice. Host BALB/c mice were imaged using IVIS 3 times a week. Group one received 10 × 10⁶ T_{CD}BM alone. Group two received 10X10⁶ T_{CD}BM along with 2X10⁵ B-ALL-luc cells (T_{CD}BM + B-ALL^{luc}). Group three was transplanted with 10X10⁶ T_{CD}BM and 1X10⁶ purified WT CD8⁺ T cells +1X10⁶ CD4⁺ T cells, and 2X10⁵ B-ALL-luc cells (T_{CD}BM + B-ALL^{luc} + WT CD8+CD4). Group four received 10X10⁶ T_{CD}BM and 1X10⁶ purified CD8⁺ T cells +1X10⁶ CD4⁺ T cells from SLP76 Y145FKI Eomes-sufficient mice along with 2X10⁵ B-ALL-luc cells (T_{CD}BM + B-ALL^{luc} + SLP75Y145FKI CD8+CD4). Group five received 10X10⁶ T_{CD}BM and 1X10⁶ CD8⁺ T cells +1X10⁶ CD4⁺ purified T cells from SLP76 Y145FKI Eomes-deficient mice along with 2X10⁵ B-ALL-luc cells (T_{CD}BM + B-ALL^{luc} + SLP75Y145FKI Eomes-cKO CD8+CD4). Group six received 10X10⁶ T_{CD}BM and 1X10⁶ CD8⁺ T cells +1X10⁶ CD4⁺ purified T cells from WT Eomes-deficient mice along with 2X10⁵ B-ALL-luc cells (T_{CD}BM + B-ALL^{luc} + WT Eomes cKO CD8+CD4). (E–G) (E) The mice were monitored for survival, (F) body weight changes, and (G) clinical score for 50 days post-BMT. For weight changes and clinical score, one representative of 2 independent experiments is shown (n = 3 mice/group for BM alone; n = 5 experimental mice/group for all three groups). The survival groups are a combination of all experiments. (H) We have quantitated luciferase bioluminescence of tumor growth. Statistical analysis for survival and the clinical score was performed using log calculation. Two-way ANOVA was used for statistical analysis and results were confirmed by students t-test, p values are presented. Note: Controls are naive for tumor but transplanted with 10 × 10⁶ T cell depleted bone marrow alone (T_{CD}BM) and used as a negative control for BLI. See also Figure S4.

Eomes is required for cytotoxicity and GVL effect by both SLP76Y145FKI and WT T cells

The IMP (IMP: CD44^{hi}CD122^{hi}Eomes^{hi}) (Mammadli et al., 2020; Huang et al., 2013) of SLP76Y145FKI CD8⁺ and CD4⁺ T cells arises in the thymus during development, as opposed to memory CD8⁺ and CD4⁺ T cells that are also CD44^{hi}, but largely arise in the periphery of WT mice in response to foreign antigens or due to homeostatic proliferation (Weinreich et al., 2010). We examined pre-transplanted CD4⁺ and CD8⁺ T cells for the CD44 and CD122 phenotype, and CD8⁺ T cells for CD44, CD122, and Eomes expression, and observed that SLP76Y145FKI T cells expressed higher levels of CD44, CD122, and Eomes compared to CD8⁺ T cells from WT mice (Figures 3A and 3B).

To further investigate the role of Eomes in tumor clearance and cytotoxic function, we crossed SLP76Y145FKI mice with Eomes^{flox/flox} mice and crossed these offspring with CD4cre to delete Eomes specifically in both CD4⁺ and CD8⁺ T cells (Jordan et al., 2008; Carty et al., 2014; Pikovskaya et al., 2016) (SLP76Y145FKI Eomes conditional knockout, SLP76Y145FKI cKO). To obtain ex vivo activated cells, we

performed similar allo-HSCT experiments as described above and used WT or SLP76Y145FKI CD8⁺ T cells with or without Eomes expression. Seven days post-transplant, donor CD8⁺ T cells were sorted as previously described by H2K^b positivity, and *in vitro* cytotoxicity assays were performed at a 40:1, 20:1, and 10:1 ratio (effector: target). We observed that donor T cells lacking Eomes from either SLP76Y145FKI or WT mice could not kill tumor targets (Figure 3C). Next, we examined the role of Eomes in the allo-HSCT model. Lethally irradiated BALB/c mice were injected intravenously with 10X10⁶ WT T cell-depleted BM cells along with 1X10⁶ FACS-sorted CD8⁺ and CD4⁺ T cells from either WT mice or SLP76Y145FKI Eomes^{fl^{ox}/fl^{ox}} (SLP76Y145FKI Eomes cKO) mice, with or without CD4cre (to delete Eomes specifically in CD4⁺ and CD8⁺ T cells), along with 2X10⁵ luciferase-expressing B-ALL-*luc* blast cells as described (Cheng et al., 2016). Recipient animals transplanted with WT T cells cleared the tumor cells but developed acute GVHD (Figure 3D). Recipient animals transplanted with Eomes sufficient (Eomes^{fl^{ox}/fl^{ox}} mice without CD4cre) SLP76Y145FKI T cells cleared the tumor without showing signs of GVHD (Figure 3D). These animals were monitored for survival (Figure 3E) and weight loss (Figure 3F). Recipient animals were also evaluated for clinical score 2–3 times per week by a scoring system that sums changes in 6 clinical parameters: (1) weight loss, (2) posture, (3) activity, (4) fur texture, (5) diarrhea, and (6) skin integrity (Cooke et al., 1996). Animals that lost ≥30% of their initial body weight were euthanized (Figure 3G). The bioluminescence data were analyzed and quantified with Living Image Software (Xenogen) and Igor Pro (Wave Metrics, Lake Oswego, OR) (Figure 3H). Notably, recipient animals transplanted with Eomes-deficient (Eomes^{fl^{ox}/fl^{ox}} mice with CD4cre, called SLP76Y145FKI Eomes cKO) T cells could not clear the tumor, and all died from tumor burden. Recipient animals transplanted with WT Eomes-deficient (Eomes^{fl^{ox}/fl^{ox}} mice with CD4cre, called WT Eomes cKO) T cells developed severe GVHD and were also unable to clear transplanted leukemia cells. We have confirmed the deletion of Eomes using the Eomes^{fl^{ox}/fl^{ox}} CD4 cre mice by flow cytometry (Figure S4). These data provided further evidence that Eomes is required for the GVL effect.

SLP76Y145/ITK signaling is required for T cell migration to the GVHD target tissues

GVHD involves early migration of alloreactive donor T cells into the target organs, followed by T cell expansion and tissue destruction (Ferrara, 2014). Modulation of alloreactive T cell trafficking has been suggested to play a significant role in ameliorating experimental GVHD (Lu et al., 2010). Therefore, we examined the trafficking of donor T cells to GVHD target tissues, as previously described (Lu et al., 2010). Irradiated BALB/c recipient mice were injected with CD8⁺ and CD4⁺ T cells from C57Bl/6 background SLP76Y145FKI (CD45.2⁺) and WT B6LY5 (CD45.1⁺) mice mixed at a 1:1 ratio (Figure 4A), and seven days post-transplantation, recipient mice were examined for the presence of donor CD8⁺ and CD4⁺ T cells in the spleen, lymph nodes, liver, and small intestines (SIs). While the WT: SLP76Y145FKI T cell ratio for both CD8⁺ and CD4⁺ cells remained approximately 1:1 in the spleen and lymph nodes (Figures 4B and 4C), this ratio in the liver and small intestine was significantly elevated, suggesting that SLP76Y145FKI CD8⁺ and CD4⁺ T cells were defective in migration to and expansion in those tissues (Figures S5A and S5B). Using histological staining for H&E, we also observed significant leukocyte infiltration into GVHD target organs such as liver, skin, and SI (Cho et al., 2020), in WT T cell recipients but not in SLP76Y145FKI T cell recipients (Figure 4D).

Pro-inflammatory conditioning treatment may promote donor T cell migration into GVHD target tissues (Wysocki et al., 2004; Seif et al., 2017). We therefore examined if the observed defect in trafficking was due to chemokine receptor expression on donor T cells. Irradiated BALB/c recipient mice were injected with WT and SLP76Y145FKI CD8⁺ and CD4⁺ T cells as described previously, and at seven days post-transplantation, donor CD4⁺ and CD8⁺ T cells were FACS sorted from the recipient using H2K^b expression. Purified donor CD4⁺ and CD8⁺ T cells were examined for chemokine receptor expression by qPCR. Indeed, we found that expression of chemokine receptors and other molecules that play a critical role in T cell migration (CXCR3, CX3r1, CXCR1, CCR12, s1pR1, CrTAM, CXCR6, CCR9, CXCR5, CXCR4) were significantly reduced in SLP76Y145FKI CD8⁺ and CD4⁺ T cells at day 7 post-transplantation compared to WT CD8⁺ and CD4⁺ T cells (Figures 4E and 4F).

As an alternative approach, we tracked both CD8⁺ and CD4⁺ T cells in allo-BMT mice by using donor CD8⁺ and CD4⁺ T cells from WT and SLP76Y145FKI mice that also express luciferase, which could be monitored by bioluminescence (Negrin and Contag, 2006). We observed that both CD8⁺ and CD4⁺ donor T cells from SLP76Y145FKI mice had significantly impaired residency in GVHD target organs—including the liver and SI—compared to WT, despite no differences in spleen and lymph nodes (Figure 4G). Luciferase bioluminescence was quantified for secondary lymphoid organs (spleen and lymph nodes) and GVHD target organs (SI and liver) (Figures S6A and S6B). These data suggest that SLP76Y145FKI CD8⁺ and CD4⁺ T cells

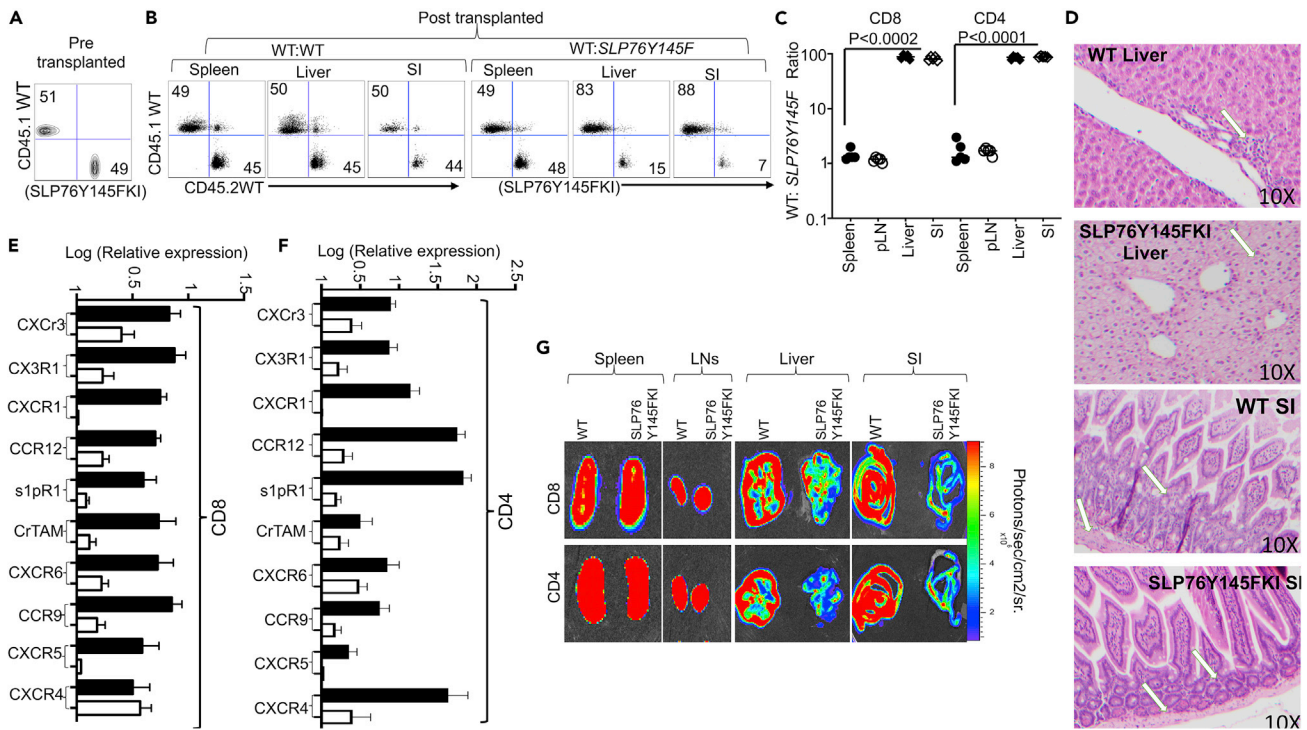


Figure 4. SLP76Y145/ITK signaling is required for T cell migration to the GVHD target tissues

(A) Irradiated BALB/c mice were allo-transplanted and injected with FACS-sorted CD8⁺ or CD4⁺ T cells mixed at a 1:1 ratio from WT B6.SJL (Ly5 CD45.1) and WT C57B16 (CD45.2) mice. We also transplanted FACS-sorted CD8⁺ or CD4⁺ T cells from B6.SJL (Ly5 CD45.1) and SLP75Y145FKI (C57B16 in background, CD45.2) mice at a 1:1 ratio. FACS analysis of sorted T cells pre-transplant is shown.

(B and C) On day seven post-transplantation, the spleen, liver, and small intestine (SI) from recipients were examined for donor CD4 and CD8⁺ T cells by H2K^b CD45.1⁺ (LY5) or CD45.2⁺ (B6). We also examined donor CD4 or CD8⁺ T cells from WT mice by H2K^b CD45.1⁺, and from SLP75Y145FKI mice by H2K^b and CD45.2⁺. The ratio of WT: SLP75Y145FKI CD8⁺ and CD4⁺ T cells in the organs was determined.

(D) We transplanted either CD4⁺ or CD8⁺ T cells separately into irradiated BALB/c mice, in separate experiments. At day 7 post-allo-HSCT, liver and small intestines were examined by H&E staining (10X magnification).

(E and F) On Day 7 post-allo-HSCT, donor CD8⁺ or CD4⁺ T cells from separate experiments were isolated and examined for the expression of CXCr3, CX3r1, CXCr1, CCR12, s1pR1, CrTAM, CXCR6, CCR9, CXCR5, and CXCR4 using q-PCR. p values were calculated using two-way ANOVA and Student's t test, p values are listed.

(G) Irradiated BALB/c mice were BM-transplanted and injected with CD8⁺ T cells and CD4⁺ T cells from luciferase-expressing WT or SLP75Y145FKI mice (C57Bl/6 background). On day 7 post-allo-HSCT, recipient BALB/c mice were injected with D-luciferin. Spleen, lymph nodes, liver, and small intestine were examined for donor CD8⁺ T cells or CD4⁺ T cells by luciferase expression. One representative of 2 independent experiments is shown (n = 3 mice/group for control, n = 5 mice for WT, and n = 5 mice for SLP75Y145FKI. p values were calculated using two-way ANOVA and Student's t test, p values are listed). See also Figures S5 and S6.

display attenuated chemokine receptor expression, which correlates with defective migration to GVHD target organs and reduced target organ pathology.

Novel peptide inhibitor SLP76pTYR specifically targets ITK signaling and enhances Treg cell development

Since T cells from SLP76Y145FKI mice can separate GVHD from GVL, we sought to determine whether disruption of ITK signaling with pharmacological agents would have a similar effect. When we used several commercially available small molecule inhibitors, including 10n (Carson et al., 2015; Riether et al., 2009), CTA056 (Guo et al., 2012), and GSK2250665A (Alder et al., 2013), we observed that these small molecules also inhibit several other kinases including mTOR and AKT, suggesting that these molecules were not specific (Figures S7A–S7F). Thus, we sought to design a novel inhibitor that would explicitly target the SLP76-ITK interaction and signaling by preventing the SH2 domain of ITK from docking onto SLP76 at tyrosine 145. Since evolution usually selects 7 residues at specific protein:protein interfaces for certain properties (Pletneva et al., 2006), we analyzed the physico-chemical and structural properties of the interface of the SH2 domain and SLP76-pY145 in our quest to generate a potent inhibitor of the ITK-SH2 domain:

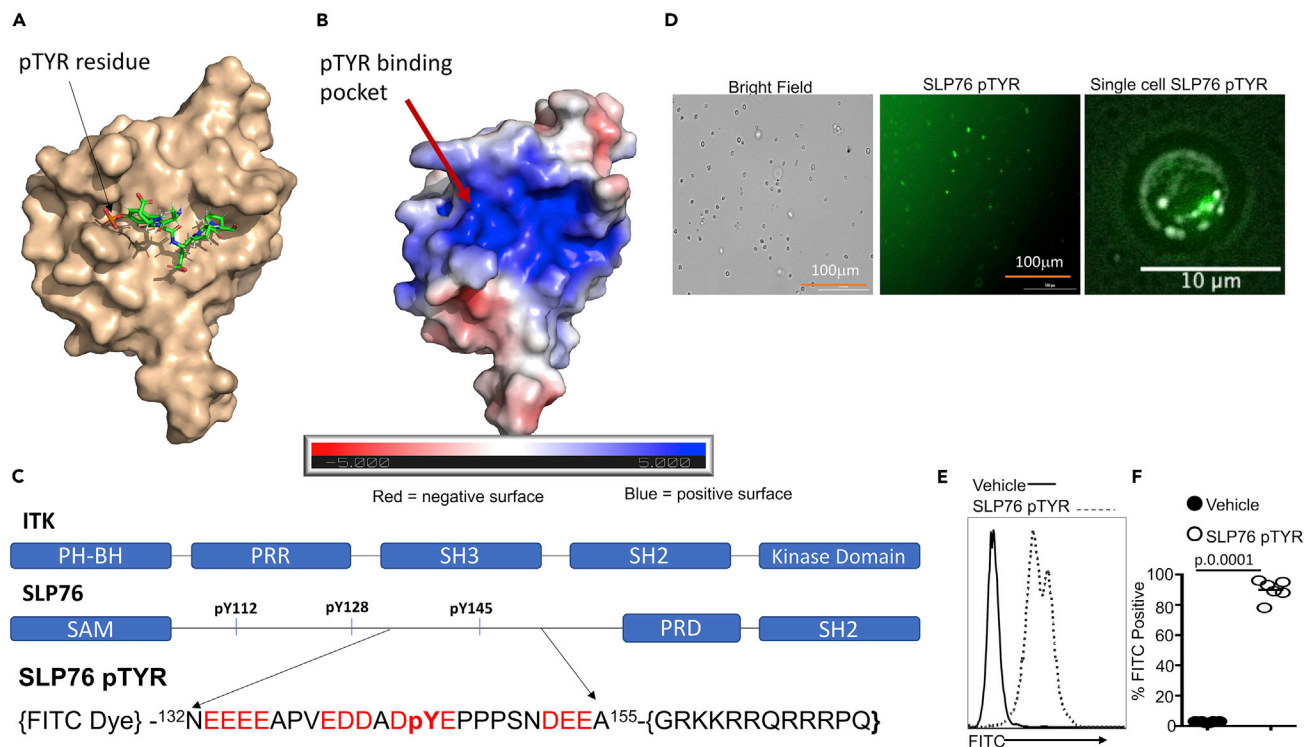


Figure 5. Development of a novel peptide that disrupts the interaction between SLP76 and ITK

(A) NMR spectroscopy structure of murine ITK SH2 domain showing its complex with a peptide containing a pTyr residue (PDB code:2ETZ) that was previously solved by Pletneva et al. (46). The SH2 domain is rendered in surface representation (wheat), while the peptide derived from residues 143–148 of SLP76 with a sequence (¹⁴³ADpYEPP¹⁴⁸) is shown in stick model. In contrast, our SLP76pTYR inhibitor consists of residues 132–155 of SLP76.

(B) Electrostatic profile is shown, calculated using the APBS plugin in Pymol.

(C) Top: Organization of the domain architecture of full-length ITK showing the c-terminal Kinase domain, Src-homology 2 (SH2), the Src-homology 3 (SH3) domains, the intrinsically disordered proline-rich region (PRR), and the N-terminal Pleckstrin homology (PH) and Tec homology (TH) domains. Bottom: Organization of the domain architecture of full-length SLP76 adaptor protein showing the N-terminal SAM domain, the intrinsically disordered region containing phosphotyrosines pY112, pY128, pY145, which are followed by a proline-rich domain (PRD) and a C-terminal SH2 domain. Bottom: Design of the novel peptide, SLP76pTYR with an N-terminal FITC to monitor the peptide in cells and a C-terminal TAT sequence (GRKKRRQRRRPQ TAT sequences) for cell membrane permeability. Also shown are the amino acid sequence of residues 132–155 of SLP76, which was used to design the SLP76pTYR peptide inhibitor.

(D) T cells were examined for percentage FITC positive by fluorescence microscopy. A single cell in focal plane near the cover glass was imaged.

(E) Primary cells cultured with SLP76pTYR or the non-specific peptide were washed and examined for FITC expression by flow cytometry.

(F) Quantification of the FITC expression for (E). We used two-way ANOVA for statistical analysis and confirmed our statistical finding by Student's t-test was performed. See also Figure S7.

SLP76-pY145 interaction (Figures 5A and 5B). We examined the Y145 region of SLP76 to design a short peptide that can inhibit ITK via competitive binding. In addition, to avoid the unintended non-specific binding of our peptide to the more than hundred other SH2 domains (and/or to other unexpected targets) *in vivo* (Andersen et al., 2019), we incorporated as many distinctive features of the SLP76 region around the pY145 as possible. We used the previously published atomic-resolution NMR spectroscopy structures of the SH2 domain of ITK, free and in complex with a short peptide containing a pTyr residue (Pletneva et al., 2006), as a guide (Figure 5A). The SH2 domain of ITK contains a complementary electrostatic surface, because the phosphotyrosine binding pocket, as well as the surrounding surface groove, is highly positively charged, suggesting that electrostatics most likely will play a vital role in this interaction (Figure 5B). These efforts led to the design of a novel SLP76pTYR peptide predicted to bind to the ITK SH2 domain and prevent ITK from docking onto SLP76 at the tyrosine at 145 position (Figure 5C). BLASTing (Altschul et al., 1990) the peptide sequence of our novel peptide SLP76145pTYR against the non-redundant human proteome showed minimal identity with other proteins, suggesting that the interaction between SLP76pTYR and the SH2 domain is unique, and most likely will be specific toward ITK signaling. The SLP76pTYR construct consists of two components (Figure 5C): (i) amino acid residues 132 to 155 of SLP76 with phosphorylated tyrosine at position 145 and (ii) a TAT peptide sequence (GRKKRRQRRRPQ) for cell membrane penetration (i.e. ¹³²NEEEEAPVEDDADpYEPPPSNDEEA¹⁵⁵-TAT). To test the effect of this construct to inhibit the

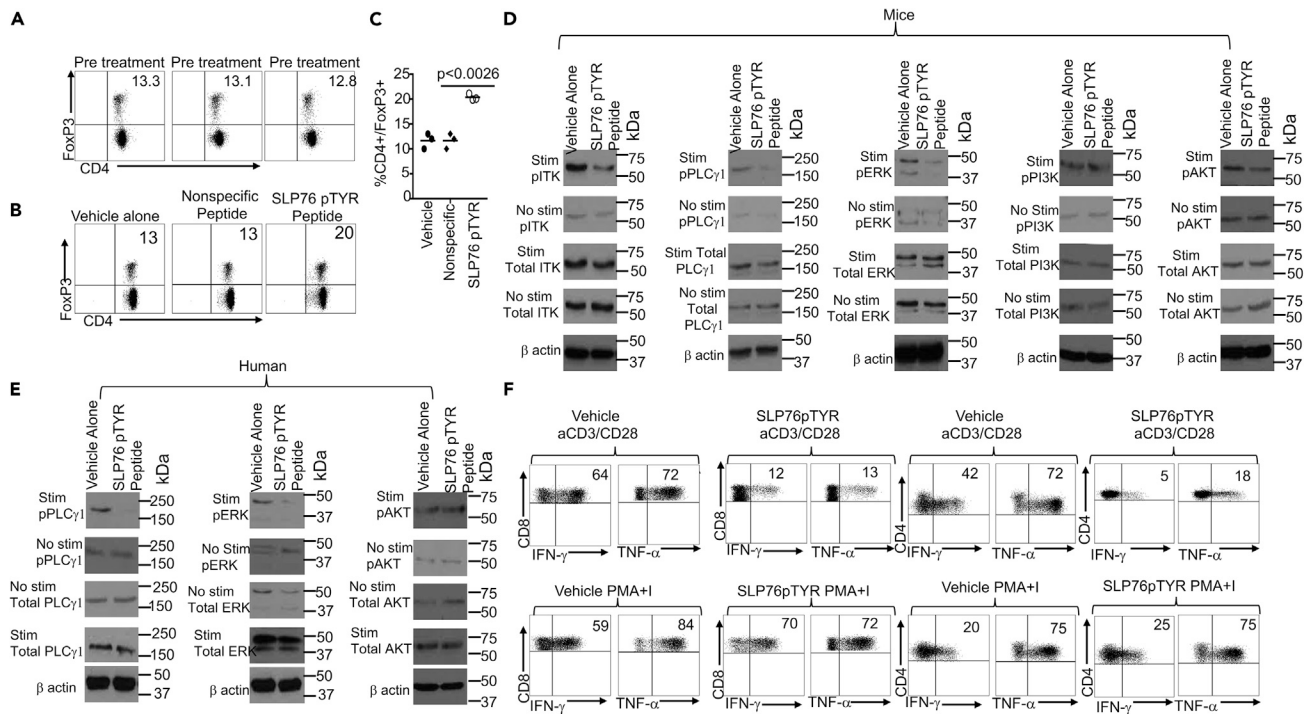


Figure 6. Novel peptide SLP76pTYR specifically targets SLP76:ITK signaling and enhances Treg cell development

(A) Murine CD4⁺ T cells were examined for total CD4⁺ and FOXP3 expression prior to treatment with SLP76pTYR. n = 3, and one representative experiment is shown.

(B) Total T cells stimulated in the presence of SLP76pTYR, nonspecific peptide, or vehicle alone were examined for total CD4 cells that are FoxP3⁺. n = 3, and one representative experiment is shown.

(C) Quantification of three experiments as in (A).

(D) Cell lysates were obtained from mouse T cells stimulated with anti-CD3 and anti-CD28 in the presence of SLP76pTYR, or vehicle alone. Lysate from stimulated cells and non-stimulated cells were examined for phosphorylated ITK, total ITK (size 50–75kDa), phosphorylated PLCγ1, total PLCγ1 (size ~155kDa), phosphorylated ERK, total ERK (size ~42kDa), phosphorylated PI3K, total PI3K, (size ~85kDa), phosphorylated AKT, and total AKT (size ~60kDa). n = 3 and one representative experiment is shown.

(E) Cell lysates from human T cells, non-stimulated or stimulated with OKT3 for 5 min in the presence of SLP76pTYR or vehicle alone, were examined for phosphorylated pPLCγ1 and total PLCγ1 on stimulated and non-stimulated T cells. Cell lysate from stimulated and non-stimulated cells were examined for pERK and total ERK. Lysates from stimulated and non-stimulated were also examined for phosphorylation and total AKT. n = 3 and one representative experiment is shown.

(F) Primary human T cells from PBMCs were stimulated with anti-CD3 and anti-CD28, or with PMA/Ionomycin, for 6 hr in the presence of vehicle alone or SLP76pTYR in the presence of Brefeldin A (BFA) (Webb et al., 2015). Intracellular IFN-γ and TNF-α expression by CD8⁺ and CD4⁺ T cells was determined by flow cytometry. For statistical analysis we used two-way ANOVA and Student's t test. p values are presented. See also Figure S8.

interaction of ITK and SLP76, we cultured T cells with a FITC-conjugated SLP76pTYR peptide, vehicle, or nonspecific peptide, and examined the cells for FITC uptake using microscopy and flow cytometry. We observed that significant numbers of cells were positive for FITC following treatment with the SLP76pTYR peptide (Figures 5D–5F). The peptide was localized in specific locations in the cell as observed by imaging the cells in a single focal plane near the cover glass. This result would be expected if the peptide were binding to ITK in signalosomes in the cell (Figure 5D).

ITK deficiency is known to enhance the development of regulatory T cells (Tregs) (Elmore et al., 2020; Owen et al., 2019) so we tested the peptide inhibitor to determine whether inhibition of the ITK:SLP76Y145 interactions using SLP76pTYR would induce Tregs. First, we examined the frequency of Tregs by expression of CD4⁺ and FoxP3⁺ (Figure 6A). Next, total mouse T cells were stimulated with anti-CD3 (Sugie et al., 2004) in the presence of either SLP76pTYR, non-specific peptide, or vehicle alone for 5 to 24 hr, and cells were harvested and examined for the presence of Tregs (CD4⁺CD25⁺FoxP3⁺). We observed significantly enhanced differentiation of Treg cells in T cell cultures treated with SLP76pTYR peptide compared to vehicle alone or nonspecific peptide (Figures 6B and 6C). Next, we stimulated mouse T cells with anti-CD3 and anti-CD28 for 5 min, in the presence of SLP76pTYR or vehicle alone, and observed a reduction in ITK phosphorylation.

We did not observe a reduction in non-stimulated phosphorylation ITK, nor did we observe any reduction for non-stimulated total ITK or stimulated total ITK. Similarly, we only observed a reduction in stimulated phosphorylation PLC γ -1; we did not observe any reduction with non-stimulated phospho-PLC γ -1 or either stimulated or non-stimulated PLC γ -1. We also observed similar effects on ERK as those we observed in ITK and PLC γ -1 (Figures 6D and S8A–S8C). We did not observe any differences in the phosphorylation of PI3K or AKT, either stimulated and non-stimulated, or on total PI3K and AKT (Figures 6D, S8D, and S8E). Next, we investigated the effects of SLP76pTYR peptide on human PBMC samples from healthy human patients. T cells from these patients were stimulated with anti-CD3 (OKT3) (Karimi et al., 2005) for 5 min in the presence of SLP76pTYR or vehicle alone. We observed reduced phosphorylation of PLC γ 1 and ERK, in stimulated T cells (Figure 6E). We did not observe any differences in non-stimulated phospho PLC γ 1 and ERK (Figures 6E, S8F, and S8G). We also did not observe any differences in total AKT or either stimulated or unstimulated phospho AKT. We also did not observe any differences in stimulated or unstimulated total human AKT (Figures 6E and S8H), providing evidence that the SLP76pTYR peptide has an impact on signaling pathways downstream of SLP76 in both mouse and human T cells. Notably, SLP76pTYR peptide exhibited minimal off-target effects against other kinases, including PI3K and AKT (Figures S8A–S8H). It is possible that PI3K and AKT lie downstream of ITK, but that the specific pathways affected by the disruption of the SLP76:ITK interaction does not affect the activation of PI3K and AKT. These data provide further evidence that our peptide affects early T cells signaling (Figure 6E). Next, we investigated the ability of SLP76pTYR peptide to affect the production of proinflammatory cytokines in human PBMCs. T cells from healthy human were stimulated with anti-CD3 (OKT3) and anti-CD28 in the presence of SLP76pTYR or vehicle alone, along with Brefeldin A. We also examined T cells incubated with SLP76pTYR or vehicle alone in the presence of PMA + Ionomycin and Brefeldin A for 6 hr. Our data show that T cells stimulated with anti-CD3/anti-CD28 had significantly reduced IFN- γ and TNF- α production when incubated in the presence of SLP76pTYR compared with the vehicle alone (Figure 6F).

Inhibition of SLP76-ITK interaction and signaling by the peptide SLP76pTYR allows tumor clearance without inducing GVHD

Next, we examined whether our peptide can inhibit SLP76:ITK interaction *in vivo* and separate GVL from GVHD as proof of principle for the approach. WT CD8⁺ and CD4⁺ T cells were mixed at a 1:1 ratio and transduced with a retrovirus carrying SLP76pTYR-pCherry or empty vector. Lethally irradiated recipient BALB/c mice were transplanted with 10×10^6 T cell-depleted BM ($T_{CD}BM$) as described, alone or together with WT CD8⁺ and CD4⁺ T cells transduced with SLP76pTYR-pCherry or empty vector-carrying virus. Recipient mice were also given 1×10^5 primary B-ALL-luc tumor cells as described (Cheng et al., 2016). While tumor growth was observed in $T_{CD}BM$ -transplanted mice that did not receive donor T cells, tumor growth was not seen in mice transplanted with either untransduced T cells, or T cells transduced with either empty viruses or SLP76pTYR-pCherry carrying viruses. Notably, mice transplanted with untransduced T cells or T cells transduced with empty virus suffered from GVHD, while mice transplanted with T cells transduced with SLP76pTYR-pCherry carrying virus survived for >40 days post-HSCT without tumor growth, with minimal signs of GVHD (Figures 7A–7E). Tumor growth was observed in only 1 out of 9 mice in the group that received the T cells transduced with SLP76pTYR-pCherry carrying virus (Figure 7F).

Altogether, these data demonstrate that disruption of SLP76:ITK signaling can separate GVHD from GVL. Inhibition of ITK signaling by SLP76pTYR, by specifically targeting the SLP76 and ITK interaction, allows tumor clearance and minimizes development of GVHD. Finally, our novel peptide inhibitor of ITK is specific and has the potential to be used in a clinical setting for T cell-mediated disorders. (Summary Figure)

DISCUSSION

This report shows that targeting the SLP76:ITK interaction and its downstream factors significantly suppresses GVHD pathogenesis while maintaining GVL effects in an allo-HSCT model. Since GVHD is primarily caused by donor T cells, modulating donor T cells by specifically targeting kinase activity will enable us to separate GVHD from GVL. Our data suggest that the SLP76:ITK signaling pathway could represent a potential target for the separation of GVHD and GVL responses after allo-HSCT.

The adapter protein SLP76 plays an essential role in regulating T cell activation downstream of the TCR by assembling a multimolecular signaling complex that includes ITK. The phosphorylation of SLP76 at Y145 leads to the activation and recruitment of ITK, which phosphorylates PLC γ 1, leading to its activation, mobilization of calcium, and activation of the NFAT transcription factor (Sahu and August, 2009). T cells that carry

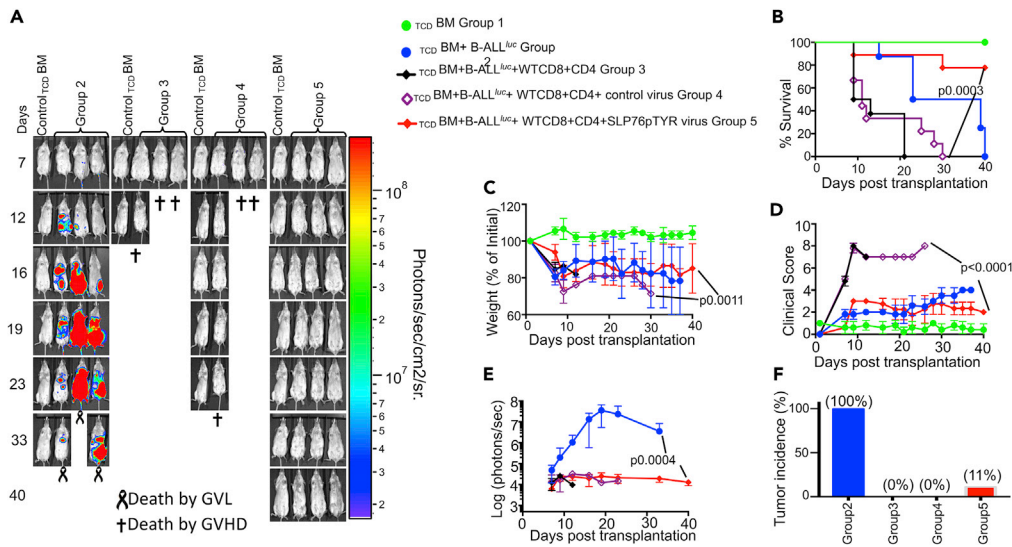


Figure 7. Inhibition of T cells by the peptide SLP76pTYR allows tumor clearance without inducing GVHD

(A) Purified WT CD8⁺ and CD4⁺ T cells were mixed (1X10⁶ total) at a 1:1 ratio, and transduced with viruses containing SLP76pTYR or empty vector, then transplanted along with 1X10⁵ B-ALL-*luc* cells and 5 × 10⁶ T cell-depleted bone marrow cells into irradiated BALB/c mice. Host BALB/c mice were imaged using IVIS 200 3 times a week. Group one received 10 × 10⁶ T cell-depleted bone marrow alone (T_{CD}BM). Group two received 10X10⁶ T_{CD}BM along with 1X10⁵ B-ALL-*luc* cells (T_{CD}BM + B-ALL^{luc}). The third group was transplanted with 10X10⁶ T_{CD}BM and a 1:1 ratio of purified WT CD8⁺ and CD4⁺ T cells (1X10⁶ total) along with 1X10⁵ B-ALL-*luc* cells (T_{CD}BM + B-ALL^{luc} + WT CD8+CD4). Group four received 10X10⁶ T_{CD}BM and a 1:1 ratio of purified WT CD8⁺ and CD4⁺ T cells (1X10⁶ total) transduced with control viruses along with 2X10⁵ B-ALL-*luc* cells (T_{CD}BM + B-ALL^{luc} + Empty CD8+CD4). Group five received 10X10⁶ T_{CD}BM, a 1:1 ratio of purified WT CD8⁺ and CD4⁺ T cells (1X10⁶ each) transduced with SLP76pTYR-carrying viruses, and with 1X10⁵ B-ALL-*luc* cells (T_{CD}BM + B-ALL^{luc} + SLP76pTYR virus CD8+CD4).

(B–D) (B) The mice were monitored for survival, (C) body weight changes, and (D) clinical score for 40 days post BMT. For weight changes and clinical score, one representative of 2 independent experiments is shown (n = 3 mice/group for BM alone; n = 5 experimental mice/group for all three groups).

(E) Quantitated luciferase bioluminescence of tumor growth.

(F) Tumor incidence for each of the experimental groups.

Statistical analysis for survival and clinical score was performed using log rank test and two-way ANOVA, respectively.

Note: Controls are naive for tumor, but transplanted with 10 × 10⁶ T cell depleted bone marrow alone (T_{CD}BM) and used as a negative control for BLI.

a Y145F mutation in SLP76 fail to phosphorylate and activate PLCγ1 in response to TCR stimulation (Jordan et al., 2008). Although T cells expressing the SLP76 Y145F mutation exhibit signaling defects downstream of TCR stimulation, not all T cell functions are lost when ITK recruitment and activation is defective. For example, SLP76Y145FKI mice can clear acute LCMV infection (Smith-Garvin et al., 2010). The ability of T cells from SLP76Y145FKI mice to induce GVL without GVHD indicates that the SLP76:ITK pathway controls these functions. Several groups have reported that both naive CD44^{lo} CD4⁺ and CD8⁺ T cells can induce lethal GVHD, while CD44^{hi} T cells do not (Dutt et al., 2011). Since a high proportion of CD4⁺ and CD8⁺ T cells from SLP76 Y145F mice are CD44^{hi} and CD122^{hi} and express higher levels of Eomes (IMP phenotype) (Weinreich et al., 2010), we investigated the capacity of this IMP population to induce GVHD and GVL compared to CD8⁺ and CD4⁺ CD44^{lo}CD122^{lo} T cell populations in our allo-HSCT model. We found that WT CD8⁺ and CD4⁺, CD44^{lo}CD122^{lo} T cells induced acute GVHD, while CD8⁺ and CD4⁺ with IMP phenotype had reduced ability to do so, with significantly delayed induction of GVHD. However, animals eventually succumbed to the symptoms of GVHD, confirming previous reports (Zhang et al., 2005). Although the SLP76Y145F mice exhibit defects in the development of other T cells in addition to the IMP cells, such as iNKT (Gerth and Mattner, 2019; Muro et al., 2019) cells and gamma delta T cells (Muro et al., 2019; Navas et al., 2017), we have specifically focused on the role of CD8⁺ and CD4⁺ T cells in GVL vs. GVHD. We also noted that both CD8⁺ and CD4⁺ SLP76Y145FKI T cells with IMP phenotype as well as those lacking the IMP phenotype exhibit GVL with reduced capacity to induce GVHD. It is likely that the altered signaling experienced by the cells with the SLP76Y145FKI mutation allows these cells to be able to have anti-tumor activity in a T cell-intrinsic manner.

Recently, several convergent lines of evidence have suggested that inflammatory cytokines act as mediators of acute GVHD (Lynch Kelly et al., 2015; Holler, 2002; Ju et al., 2005). Therefore, we investigated whether donor T cells with attenuated TCR signaling might reduce cytokine storm mediated by donor T cells. Our data showed that both CD8⁺ and CD4⁺ T cells from WT C57Bl/6 mice (MHC haplotype b) produced significantly higher cytokines both on a serum and a cellular level when transplanted into BALB/c mice. In contrast, both donor CD8⁺ and CD4⁺ T cells from SLP76 Y145FKI C57Bl/6 mice produced significantly less cytokines on both a serum and a cellular level. Both donor CD8⁺ and CD4⁺ T cells from SLP76 Y145FKI also exhibited reduced expression of chemokine receptors compared to WT donor T cells. The defective migration of donor CD8⁺ and CD4⁺ SLP76Y145FKI T cells likely contributes to the attenuation of GVHD. The retention of T cells in secondary lymphoid organs by FTY720-mediated inhibition of S1PR1 also ameliorates GVHD while maintaining GVL effects (Villarreal et al., 2014; Liu et al., 2012). The chemokine receptor CXCR3 has an important role in the migration of effector T cells in GVHD model (Duffner et al., 2003). CX3r1, CXCR1, CCR12, CrTAM, CXCR6, CCR9, CXCR5, and CXCR4 have been shown to play a significant role in donor T cell migration to GVHD target organs (Barrett, 2015; Castor et al., 2012; Hsiao et al., 2020). In a clinical study, blockade of these chemokine receptors by a small molecule antagonist led to a reduction in GVHD with no significant difference in relapse rates, suggesting that blocking T cell migration to target tissues could reduce GVHD severity without compromising the beneficial GVL effect (Vadakekolathu and Rutella, 2017). Activated alloreactive CD8⁺ T cells upregulate the expression of CX3CR1 and CXCR6 after allo-HSCT (Duffner et al., 2003; Vadakekolathu and Rutella, 2017), and these receptors are important for the homing of CD8⁺ T cells to the liver and intestines. Thus, CXCR6 deficiency or blockade of the CXCR3 and CXCR6 ligands attenuates GVHD (Duffner et al., 2003), and importantly, the GVL effect is still maintained under these conditions (Sato et al., 2005). Thus, blocking T cell migration by chemokine receptor blockade could be beneficial in the treatment of GVHD after allo-HSCT. We have also demonstrated as a proof of concept that specific targeting of the SLP76: ITK interactions can be achieved to potentially differentially modulate GVL and GVHD by pharmacologic agents. Rather than directly inhibiting the activity of the kinase domain of ITK, which could result in complete blockage of all ITK kinase activity in T cells (and potentially non-specifically affect other tyrosine kinases), we developed a strategy to specifically disrupt the SLP76-pY145-mediated activation of ITK function in T cells. The interaction between ITK and SLP76 involves the phospho-tyrosines at position pY145 and the proline-rich domain (PRD) of SLP76 docking onto the SH2 and SH3 domains of ITK, respectively. This multivalent anchoring of ITK on the different SLP76 docking sites results in distinct downstream signaling effects (Grasis et al., 2010). Previous work from Grasis et al. has shown that blocking the interaction between the PRD of SLP76 and SH3 domain of ITK, using a peptide mimicking the PRD of SLP76, inhibited the TCR-induced association between ITK and SLP-76 and the transphosphorylation of ITK, as well as actin polarization at the T-cell contact site and expression of Th2 cytokines (Grasis et al., 2010). Based on our findings that SLP76Y145FKI mutant T cells can mediate tumor clearance through GVL without inducing unwanted GVHD effects, we took advantage of this fact and blocked the SLP76 pY145-mediated docking of ITK through its SH2 domain. Thus, converting Y145 to F145 in SLP76 or preventing SH2 docking by our novel SLP76145pTYR peptide does not entirely abolish the interaction between SLP76 and ITK, but significantly affects ITK kinase activity and results in severe defects in specific downstream signaling pathways (Andreotti et al., 2010). Targeting this specific interaction would therefore retain signaling pathways that maintain GVL effects but ameliorate GVHD. When we utilized the SLP76pTYR peptide to specifically target ITK signaling, we observed specific effects only on ITK signaling, without significant effects on other tyrosine kinases. Furthermore, SLP76pTYR inhibition of ITK signaling also enhances Tregs frequency *in vitro*, confirming the peptide's ability to affect ITK signaling and T cell effector functions. We recently reported similar effects using a model of ITK deficiency (Mammadli et al., 2020).

This SLP76pTYR peptide significantly reduced IFN- γ and TNF- α production by TCR stimulated primary human T cells isolated from PBMCs. Treatment of murine donor T cells with SLP76pTYR before transfer resulted in tumor clearance without inducing GVHD. Future therapies involving our novel SLP76pTYR peptide inhibitor and small molecule inhibitors could potentially be an effective strategy for enhancing GVL while avoiding GVHD. Thus, more selective ITK inhibition using our SLP76pTYR peptide could be beneficial in the treatment of autoimmune diseases while maintaining T cell effector functions.

Limitations of the study

Currently, this study's limitation is the use of our novel peptide SLP76pTYR, which can only be used *in vitro* or as a construct to transduce T cells. We are working with structural and medicinal chemists to make our

peptide smaller and more stable, allowing it to be used for *in vivo* studies. From our *in vitro* studies, our peptide does reproduce the effects seen in SLP76Y145FKI mice.

Resource availability

Lead contact

- (1) for SLP76Y145FKI mice permission from lead contact Dr. Martha S. Jordan (University of Pennsylvania) (jordanm@mail.med.upenn.edu) is required by Material transfer Agreement (MTA) rules.
- (2) ITK-deficient mice permission from lead contact Dr. Avery August, Department of Microbiology and Immunology Cornell University College of Veterinary Medicine Ithaca, NY 14853 (aa749@cornell.edu) by MTA rules.
- (3) SLP76pTYR is patented (P38257) by The Research Foundation For The State University of New York, at SUNY Upstate Medical University Registration No. 43,497. At this point, this material is under further consideration and might not be available immediately.
- (4) For all other reagents please contact Mobin Karimi, Department of Microbiology and Immunology. MTA rules will be applied. SUNY Upstate Medical University, 766 Irving Ave Weiskotten Hall Suite 2281, Syracuse, NY 13210 (karimim@upstate.edu)

Materials availability

All resources are available to anyone by request. SLP76pTYR is under further consideration and might not be available immediately.

Data and code availability

No software products, custom code, or algorithms were developed for this manuscript.

METHODS

All methods can be found in the accompanying [transparent methods supplemental file](#).

SUPPLEMENTAL INFORMATION

Supplemental information can be found online at <https://doi.org/10.1016/j.isci.2021.102286>.

ACKNOWLEDGMENTS

We thank all members of the Karimi and August laboratories for helpful discussions. This research was funded in part by a grant from the National Blood Foundation Scholar Award to (MK) and the National Institutes of Health (NIH LRP #L6 MD0010106 and K22 (AI130182) to MK. Upstate Medical University Cancer grant (1146249-1-75632) to MK.

AUTHOR CONTRIBUTIONS

M.M., W.H., R.H., J.R., S.W., H.X., A.B., A.M., A.W., and M.K. performed experiments; W.T., Y.C., and T.G. provided valuable reagents; R.H. assisted with data analysis, experimental design, scientific discussion, and editing the manuscript; and W.H., A.A., A.B., and M.K. designed experiments, analyzed the data, and wrote the manuscript.

DECLARATION OF INTERESTS

A.A. receives research support from 3M Corporation. W.H. receives research support from Mega Robo Technologies. The other authors declare no conflicts of interest.

Received: October 13, 2020

Revised: November 27, 2020

Accepted: March 4, 2021

Published: April 23, 2021

REFERENCES

- Alder, C.M., Ambler, M., Campbell, A.J., Champigny, A.C., Deakin, A.M., Harling, J.D., Harris, C.A., Longstaff, T., Lynn, S., Maxwell, A.C., et al. (2013). Identification of a novel and selective series of itk inhibitors via a template-hopping strategy. *ACS Med. Chem. Lett.* **4**, 948–952.
- Altschul, S.F., Gish, W., Miller, W., Myers, E.W., and Lipman, D.J. (1990). Basic local alignment search tool. *J. Mol. Biol.* **215**, 403–410.
- Amir, A.L., Hagedoorn, R.S., Van Luxemburg-Heijs, S.A., Marijt, E.W., Kruisselbrink, A.B., Frederik Falkenburg, J.H., and Heemskerk, M.H. (2012). Identification of a coordinated CD8 and CD4 T cell response directed against mismatched HLA Class I causing severe acute graft-versus-host disease. *Biol. Blood Marrow Transpl.* **18**, 210–219.
- Andersen, T.C.B., Kristiansen, P.E., Huszenicza, Z., Johansson, M.U., Gopalakrishnan, R.P., Kjølstrup, H., Boyken, S., Sundvold-Gjerstad, V., Granum, S., Sorli, M., et al. (2019). The SH3 domains of the protein kinases ITK and LCK compete for adjacent sites on T cell-specific adapter protein. *J. Biol. Chem.* **294**, 15480–15494.
- Anderson, K. (2003). Broadening the spectrum of patient groups at risk for transfusion-associated GVHD: implications for universal irradiation of cellular blood components. *Transfusion* **43**, 1652–1654.
- Andreotti, A.H., Schwartzberg, P.L., Joseph, R.E., and Berg, L.J. (2010). T-cell signaling regulated by the Tec family kinase, Itk. *Cold Spring Harb. Perspect. Biol.* **2**, a002287.
- Atherly, L.O., Lucas, J.A., Felices, M., Yin, C.C., Reiner, S.L., and Berg, L.J. (2006). The Tec family tyrosine kinases Itk and Rlk regulate the development of conventional CD8+ T cells. *Immunity* **25**, 79–91.
- Barrett, A.J. (2015). A new checkpoint in the path to GVHD? How bedside-to-bench stem cell transplant studies can inform human GVHD biology. *J. Leukoc. Biol.* **97**, 213–215.
- Bastien, J.P., Roy, J., and Roy, D.C. (2012). Selective T-cell depletion for haplotype-mismatched allogeneic stem cell transplantation. *Semin. Oncol.* **39**, 674–682.
- Baxter, A.G., and Hodgkin, P.D. (2002). Activation rules: the two-signal theories of immune activation. *Nat. Rev. Immunol.* **2**, 439–446.
- Bleakley, M., Turtle, C.J., and Riddell, S.R. (2012). Augmentation of anti-tumor immunity by adoptive T-cell transfer after allogeneic hematopoietic stem cell transplantation. *Expert Rev. Hematol.* **5**, 409–425.
- Bogin, Y., Ainey, C., Beach, D., and Yablonski, D. (2007). SLP-76 mediates and maintains activation of the Tec family kinase Itk via the T cell antigen receptor-induced association between SLP-76 and Itk. *Proc. Natl. Acad. Sci. U S A* **104**, 6638–6643.
- Breems, D.A., and Lowenberg, B. (2005). Autologous stem cell transplantation in the treatment of adults with acute myeloid leukaemia. *Br. J. Haematol.* **130**, 825–833.
- Bunnell, S.C., Diehn, M., Yaffe, M.B., Findell, P.R., Cantley, L.C., and Berg, L.J. (2000). Biochemical interactions integrating Itk with the T cell receptor-initiated signaling cascade. *J. Biol. Chem.* **275**, 2219–2230.
- Carson, C.C., Moschos, S.J., Edmiston, S.N., Darr, D.B., Nikolaishvili-Feinberg, N., Groben, P.A., Zhou, X., Kuan, P.F., Pandey, S., Chan, K.T., et al. (2015). IL2 inducible T-cell kinase, a novel therapeutic target in melanoma. *Clin. Cancer Res.* **21**, 2167–2176.
- Carty, S.A., Koretzky, G.A., and Jordan, M.S. (2014). Interleukin-4 regulates eomesodermin in CD8+ T cell development and differentiation. *PLoS One* **9**, e106659.
- Castor, M.G., Pinho, V., and Teixeira, M.M. (2012). The role of chemokines in mediating graft versus host disease: opportunities for novel therapeutics. *Front. Pharmacol.* **3**, 23.
- Cheng, Y., Chikwava, K., Wu, C., Zhang, H., Bhagat, A., Pei, D., Choi, J.K., and Tong, W. (2016). LNK/SH2B3 regulates IL-7 receptor signaling in normal and malignant B-progenitors. *J. Clin. Invest.* **126**, 1267–1281.
- Cho, H.S., Ha, S., Shin, H.M., Reboldi, A., Hall, J.A., Huh, J.R., Usherwood, E.J., and Berg, L.J. (2020). CD8(+) T cells require Itk-mediated TCR signaling for migration to the intestine. *Immunohorizons* **4**, 57–71.
- Cooke, K.R., Kobzik, L., Martin, T.R., Brewer, J., Delmonte, J., Jr., Crawford, J.M., and Ferrara, J.L. (1996). An experimental model of idiopathic pneumonia syndrome after bone marrow transplantation: I. The roles of minor H antigens and endotoxin. *Blood* **88**, 3230–3239.
- D'Aveni, M., Rossignol, J., Coman, T., Sivakumaran, S., Henderson, S., Manzo, T., Santos E Sousa, P., Bruneau, J., Fouquet, G., Zavala, F., et al. (2015). G-CSF mobilizes CD34+ regulatory monocytes that inhibit graft-versus-host disease. *Sci. Transl. Med.* **7**, 281ra42.
- Duffner, U., Lu, B., Hildebrandt, G.C., Teshima, T., Williams, D.L., Reddy, P., Ordemann, R., Clouthier, S.G., Lowler, K., Liu, C., et al. (2003). Role of CXCR3-induced donor T-cell migration in acute GVHD. *Exp. Hematol.* **31**, 897–902.
- Dutt, S., Baker, J., Kohrt, H.E., Kambham, N., Sanyal, M., Negrin, R.S., and Strober, S. (2011). CD8+CD44(hi) but not CD4+CD44(hi) memory T cells mediate potent graft antilymphoma activity without GVHD. *Blood* **117**, 3230–3239.
- Elmore, J.P., Mcgee, M.C., Nidetz, N.F., Anannya, O., Huang, W., and August, A. (2020). Tuning T helper cell differentiation by Itk. *Biochem. Soc. Trans.* **48**, 179–185.
- Ferrara, J.L. (2014). Blood and marrow transplant clinical trials network: progress since the state of the science symposium 2007. *Biol. Blood Marrow Transpl.* **20**, 149–153.
- Gerth, E., and Mattner, J. (2019). The role of adaptor proteins in the biology of natural killer T (NKT) cells. *Front. Immunol.* **10**, 1449.
- Grasis, J.A., Guimond, D.M., Cam, N.R., Herman, K., Magotti, P., Lambris, J.D., and Tsoukas, C.D. (2010). In vivo significance of ITK-SLP-76 interaction in cytokine production. *Mol. Cell. Biol.* **30**, 3596–3609.
- Guinan, E.C., Boussiotis, V.A., Neuberg, D., Brennan, L.L., Hirano, N., Nadler, L.M., and Gribben, J.G. (1999). Transplantation of anergic histoincompatible bone marrow allografts. *N. Engl. J. Med.* **340**, 1704–1714.
- Guo, W., Liu, R., Ono, Y., Ma, A.H., Martinez, A., Sanchez, E., Wang, Y., Huang, W., Mazloom, A., Li, J., et al. (2012). Molecular characteristics of CTA056, a novel interleukin-2-inducible T-cell kinase inhibitor that selectively targets malignant T cells and modulates oncomirs. *Mol. Pharmacol.* **82**, 938–947.
- Henden, A.S., and Hill, G.R. (2015). Cytokines in graft-versus-host disease. *J. Immunol.* **194**, 4604–4612.
- Holler, E. (2002). Cytokines, viruses, and graft-versus-host disease. *Curr. Opin. Hematol.* **9**, 479–484.
- Hsiao, M., Tatishchev, S., Khedro, T., Yaghmour, B., O'connell, C., and Yaghmour, G. (2020). First report of severe acute graft-versus-host disease after allogeneic stem cell transplant in a patient with myelodysplastic syndrome treated with atezolizumab: literature review. *World J. Oncol.* **11**, 112–115.
- Huang, W., Hu, J., and August, A. (2013). Cutting edge: innate memory CD8+ T cells are distinct from homeostatic expanded CD8+ T cells and rapidly respond to primary antigenic stimuli. *J. Immunol.* **190**, 2490–2494.
- Huang, W., Huang, F., Kannan, A.K., Hu, J., and August, A. (2014). Itk tunes IL-4-induced development of innate memory CD8+ T cells in a gammadelta T and invariant NKT cell-independent manner. *J. Leukoc. Biol.* **96**, 55–63.
- Huang, W., Mo, W., Jiang, J., Chao, N.J., and Chen, B.J. (2019). Donor allospecific CD44(high) central memory T cells have decreased ability to mediate graft-vs.-host disease. *Front. Immunol.* **10**, 624.
- Jordan, M.S., Sadler, J., Austin, J.E., Finkelstein, L.D., Singer, A.L., Schwartzberg, P.L., and Koretzky, G.A. (2006). Functional hierarchy of the N-terminal tyrosines of SLP-76. *J. Immunol.* **176**, 2430–2438.
- Jordan, M.S., Smith, J.E., Burns, J.C., Austin, J.E., Nichols, K.E., Aschenbrenner, A.C., and Koretzky, G.A. (2008). Complementation in trans of altered thymocyte development in mice expressing mutant forms of the adaptor molecule SLP76. *Immunity* **28**, 359–369.
- Ju, X.P., Xu, B., Xiao, Z.P., Li, J.Y., Chen, L., Lu, S.Q., and Huang, Z.X. (2005). Cytokine expression during acute graft-versus-host disease after allogeneic peripheral stem cell transplantation. *Bone Marrow Transpl.* **35**, 1179–1186.
- Kambayashi, T., Larosa, D.F., Silverman, M.A., and Koretzky, G.A. (2009). Cooperation of adapter molecules in proximal signaling cascades during allergic inflammation. *Immunol. Rev.* **232**, 99–114.

- Karimi, M., Cao, T.M., Baker, J.A., Verneris, M.R., Soares, L., and Negrin, R.S. (2005). Silencing human NKG2D, DAP10, and DAP12 reduces cytotoxicity of activated CD8+ T cells and NK cells. *J. Immunol.* 175, 7819–7828.
- Kim, M., Jung, J., and Lee, K. (2009). Roles of ERK, PI3 kinase, and PLC-gamma pathways induced by overexpression of translationally controlled tumor protein in HeLa cells. *Arch. Biochem. Biophys.* 485, 82–87.
- Koretzky, G.A., Abtahian, F., and Silverman, M.A. (2006). SLP76 and SLP65: complex regulation of signalling in lymphocytes and beyond. *Nat. Rev. Immunol.* 6, 67–78.
- Liu, W., Ren, H.Y., Dong, Y.J., Wang, L.H., Yin, Y., Li, Y., Qiu, Z.X., Cen, X.N., and Shi, Y.J. (2012). Bortezomib regulates the chemotactic characteristics of T cells through downregulation of CXCR3/CXCL9 expression and induction of apoptosis. *Int. J. Hematol.* 96, 764–772.
- Loschi, M., Porcher, R., Peffault De Latour, R., Vanneaux, V., Robin, M., Xhaard, A., Sicre De Fontebrune, F., Larghero, J., and Socie, G. (2015). High number of memory t cells is associated with higher risk of acute graft-versus-host disease after allogeneic stem cell transplantation. *Biol. Blood Marrow Transpl.* 21, 569–574.
- Lu, S.X., Holland, A.M., Na, I.K., Terwey, T.H., Alpdogan, O., Bautista, J.L., Smith, O.M., Suh, D., King, C., Kochman, A., et al. (2010). Absence of P-selectin in recipients of allogeneic bone marrow transplantation ameliorates experimental graft-versus-host disease. *J. Immunol.* 185, 1912–1919.
- Lu, Y., and Waller, E.K. (2009). Dichotomous role of interferon-gamma in allogeneic bone marrow transplant. *Biol. Blood Marrow Transpl.* 15, 1347–1353.
- Lynch Kelly, D., Lyon, D.E., Ameringer, S.A., and Elswick, R.K. (2015). Symptoms, cytokines, and quality of life in patients diagnosed with chronic graft-versus-host disease following allogeneic hematopoietic stem cell transplantation. *Oncol. Nurs. Forum* 42, 265–275.
- Mammadli, M., Huang, W., Harris, R., Sultana, A., Cheng, Y., Tong, W., Pu, J., Gentile, T., Dsouza, S., Yang, Q., et al. (2020). Targeting interleukin-2-inducible T-cell kinase (ITK) differentiates GVL and GVHD in allo-HSCT. *Front. Immunol.* 11, 593863.
- Mancusi, A., Piccinelli, S., Velardi, A., and Pierini, A. (2018). The effect of TNF-alpha on regulatory T cell function in graft-versus-host disease. *Front. Immunol.* 9, 356.
- Muro, R., Takayanagi, H., and Nitta, T. (2019). T cell receptor signaling for gammadelta T cell development. *Inflamm. Regen.* 39, 6.
- Navas, V.H., Cucho, C., Alcover, A., and Di Bartolo, V. (2017). Serine phosphorylation of SLP76 is dispensable for T cell development but modulates helper T cell function. *PLoS One* 12, e0170396.
- Negrin, R.S., and Contag, C.H. (2006). In vivo imaging using bioluminescence: a tool for probing graft-versus-host disease. *Nat. Rev. Immunol.* 6, 484–490.
- Owen, D.L., Mahmud, S.A., Sjaastad, L.E., Williams, J.B., Spanier, J.A., Simeonov, D.R., Ruscher, R., Huang, W., Proekt, I., Miller, C.N., et al. (2019). Thymic regulatory T cells arise via two distinct developmental programs. *Nat. Immunol.* 20, 195–205.
- Pikovskaya, O., Chaix, J., Rothman, N.J., Collins, A., Chen, Y.H., Scipioni, A.M., Vivier, E., and Reiner, S.L. (2016). Cutting edge: eomesodermin is sufficient to direct type 1 innate lymphocyte development into the conventional NK lineage. *J. Immunol.* 196, 1449–1454.
- Pletneva, E.V., Sundd, M., Fulton, D.B., and Andreotti, A.H. (2006). Molecular details of Itk activation by prolyl isomerization and phospholigand binding: the NMR structure of the Itk SH2 domain bound to a phosphopeptide. *J. Mol. Biol.* 357, 550–561.
- Reddy, P., and Ferrara, J.L.M. (2008). *Mouse Models of Graft-Versus-Host Disease* (StemBook).
- Riether, D., Zindell, R., Kowalski, J.A., Cook, B.N., Bentzien, J., Lombaert, S.D., Thomson, D., Kugler, S.Z., Jr., Skow, D., Martin, L.S., et al. (2009). 5-Aminomethylbenzimidazoles as potent ITK antagonists. *Bioorg. Med. Chem. Lett.* 19, 1588–1591.
- Sahu, N., and August, A. (2009). Itk inhibitors in inflammation and immune-mediated disorders. *Curr. Top. Med. Chem.* 9, 690–703.
- Sato, T., Thorlacijs, H., Johnston, B., Staton, T.L., Xiang, W., Littman, D.R., and Butcher, E.C. (2005). Role for CXCR6 in recruitment of activated CD8+ lymphocytes to inflamed liver. *J. Immunol.* 174, 277–283.
- Seif, F., Khoshmirsafa, M., Aazami, H., Mohsenzadegan, M., Sedighi, G., and Bahar, M. (2017). The role of JAK-STAT signaling pathway and its regulators in the fate of T helper cells. *Cell Commun. Signal.* 15, 23.
- Smith-Garvin, J.E., Burns, J.C., Gohil, M., Zou, T., Kim, J.S., Maltzman, J.S., Wherry, E.J., Koretzky, G.A., and Jordan, M.S. (2010). T-cell receptor signals direct the composition and function of the memory CD8+ T-cell pool. *Blood* 116, 5548–5559.
- Stritesky, G.L., Jameson, S.C., and Hogquist, K.A. (2012). Selection of self-reactive T cells in the thymus. *Annu. Rev. Immunol.* 30, 95–114.
- Su, Y.W., Zhang, Y., Schweikert, J., Koretzky, G.A., Reth, M., and Wienands, J. (1999). Interaction of SLP adaptors with the SH2 domain of Tec family kinases. *Eur. J. Immunol.* 29, 3702–3711.
- Sugie, K., Jeon, M.S., and Grey, H.M. (2004). Activation of naive CD4 T cells by anti-CD3 reveals an important role for Fyn in Lck-mediated signaling. *Proc. Natl. Acad. Sci. U S A* 101, 14859–14864.
- Tugues, S., Amorim, A., Spath, S., Martin-Blondel, G., Schreiner, B., De Feo, D., Lutz, M., Guscetti, F., Apostolova, P., Haftmann, C., et al. (2018). Graft-versus-host disease, but not graft-versus-leukemia immunity, is mediated by GM-CSF-licensed myeloid cells. *Sci. Transl. Med.* 10, eaat8410.
- Vadakekolathu, J., and Rutella, S. (2017). T-cell manipulation strategies to prevent graft-versus-host disease in haploidentical stem cell transplantation. *Biomedicines* 5, 33.
- Villaruel, V.A., Okiyama, N., Tsuji, G., Linton, J.T., and Katz, S.I. (2014). CXCR3-mediated skin homing of autoreactive CD8 T cells is a key determinant in murine graft-versus-host disease. *J. Invest. Dermatol.* 134, 1552–1560.
- Webb, J.R., Milne, K., and Nelson, B.H. (2015). PD-1 and CD103 are widely coexpressed on prognostically favorable intraepithelial CD8 T cells in human ovarian cancer. *Cancer Immunol. Res.* 3, 926–935.
- Weinreich, M.A., Odumade, O.A., Jameson, S.C., and Hogquist, K.A. (2010). T cells expressing the transcription factor PLZF regulate the development of memory-like CD8+ T cells. *Nat. Immunol.* 11, 709–716.
- Wu, T., Young, J.S., Johnston, H., Ni, X., Deng, R., Racine, J., Wang, M., Wang, A., Todorov, I., Wang, J., and Zeng, D. (2013). Thymic damage, impaired negative selection, and development of chronic graft-versus-host disease caused by donor CD4+ and CD8+ T cells. *J. Immunol.* 191, 488–499.
- Wysocki, C.A., Burkett, S.B., Panoskaltis-Mortari, A., Kirby, S.L., Luster, A.D., Mckinnon, K., Blazar, B.R., and Serody, J.S. (2004). Differential roles for CCR5 expression on donor T cells during graft-versus-host disease based on pretransplant conditioning. *J. Immunol.* 173, 845–854.
- Yu, X.Z., Albert, M.H., and Anasetti, C. (2006). Alloantigen affinity and CD4 help determine severity of graft-versus-host disease mediated by CD8 donor T cells. *J. Immunol.* 176, 3383–3390.
- Zhang, Y., Joe, G., Hexner, E., Zhu, J., and Emerson, S.G. (2005). Alloreactive memory T cells are responsible for the persistence of graft-versus-host disease. *J. Immunol.* 174, 3051–3058.
- Zheng, H., Matte-Martone, C., Jain, D., Mcniff, J., and Shlomchik, W.D. (2009). Central memory CD8+ T cells induce graft-versus-host disease and mediate graft-versus-leukemia. *J. Immunol.* 182, 5938–5948.

iScience, Volume 24

Supplemental information

Targeting SLP76:ITK interaction separates

GVHD from GVL in allo-HSCT

Mahinbanu Mammadli, Weishan Huang, Rebecca Harris, Hui Xiong, Samuel Weeks, Adriana May, Teresa Gentile, Jessica Henty-Ridilla, Adam T. Waickman, Avery August, Alaji Bah, and Mobin Karimi

Supplemental Information

Transparent Methods

Mice: SLP76 Y145FKI mice were a kind gift of Dr. Martha S. Jordan (University of Pennsylvania) (Jordan et al., 2008). ROSA26-pCAGGs-LSL-Luciferase, Thy1.1 (B6.PL-Thy1a/CyJ), CD45.1 (B6.SJL-Ptprc^a Pepc^b/BoyJ) and BALB/c mice were purchased from Charles River or Jackson Laboratory. Eomes^{flox/flox}, B6.129S1, and CD4cre mice were purchased from Jackson Laboratory. Mice expressing Cre driven by the CMV promoter (CMV-Cre) were purchased from the Jackson Laboratory and crossed to ROSA26-pCAGGs-LSL-Luciferase mice (B6-luc). B6-luc mice were bred with SLP76 Y145FKI mice to create SLP76 Y145FKI luc mice. Mice aged 8-12 weeks were used, and all experiments were performed with age and sex-matched mice. Animal maintenance and experimentation were performed in accordance with the rules and guidelines set by the institutional animal care and use committees at SUNY Upstate Medical University.

Reagents, cell lines, flow cytometry: Most monoclonal antibodies for flow cytometric analysis were purchased either from eBiosciences (San Diego, CA) or Biolegend (San Diego, CA). For TCR mediated activation, we used anti-CD3 and anti-CD28. For flow cytometry analysis, we used mouse antibodies anti-CD3-FITC, anti-CD8-FITC, anti-CD4-PE anti-BrdU-APC, anti-IFN- γ -APC, anti-TNF- α -PE, anti-CD122-APC, anti-CD25-BV421, and anti-FoxP3-APC. Mice migration studies we used anti-CD45.1 APC, anti-CD45.2-PE, H2KB PerCP. Anti-CD44 Pacific Blue, anti-CD122 APC and anti-Eomes PE. Human antibodies: anti-CD3-APC, anti-CD4-PE, anti-CD8-Pacific Blue, anti-TNF- α -Pe/Cy7, anti-IFN- γ -APC/Cy7. For serum ELISAs, we used Biolegend LEGENDplex kits, some of which were custom ordered to detect both mouse and human cytokines. For bioluminescent imaging, luciferin was purchased from Gold Bio (St Louis, MO). To exclude dead cells from analyses, we used LIVE/DEAD Fixable Aqua Dead Cell staining. All flow cytometry was performed on a BD LSR Fortessa flow cytometer (BD Biosciences). Flow data were analyzed with FlowJo software (Tree Star,

Ashland, OR). T cells were purified with anti-CD8 or anti-CD4 magnetic beads using MACS columns (Miltenyi Biotec, Auburn, CA). Cells were sorted with a FACS Aria cell sorter (BD Biosciences). FACS-sorted cells showed > 95% purity. For signaling analysis, antibodies against for both human and mouse ITK, PLC γ 1, ERK, GAPDH, AKT, PI3K and β -Actin (total and/or phosphoproteins) were purchased from Cell Signaling Technology (Danvers, MA). Cells culturing reagents were purchased from Invitrogen (Grand Island, NY) and Sigma-Aldrich (St. Louis, MO), unless otherwise specified. Primary mouse B-cell acute lymphoblastic leukemia (B-ALL) blasts and primary cells (Cheng et al., 2016) were transduced with luciferase, and cultured as described previously (Edinger et al., 2003). B-ALL was chosen for this model because (1) these cells are syngeneic with BALB/c mice and allogeneic to C57Bl/6 mice, and (2) B-ALL was selected to be more related to human disease (Cheng et al., 2016).

GVHD and GVL studies: Recipient BALB/c mice (MHC haplotype d) as recipients

were lethally irradiated with 800 cGy total in two split doses of 400cGy. Bone marrow cells were harvested from mouse legs, and total bone marrow cells were incubated with CD90.2 beads, using 100ul of beads per mouse according to manufacturer protocols. We also depleted NK cells and by DX5 beads, and CD122⁺ cells with anti PE beads. Recipient mice were injected intravenously with 10X10⁶ T cell-depleted bone marrow (T_{CD}BM) cells, with or without donor T cells, either 1X10⁶ or 2X10⁶ FACS-sorted CD8⁺, CD4⁺ T cells, or CD8⁺ and CD4⁺ cells mixed at a 1:1 ratio from WT or SLP76 Y145FKI mice. For GVL experiments, primary B cell acute lymphoblastic leukemia (B-ALL, syngeneic to BALB/c and allogeneic to C57Bl/6) blasts were transduced with luciferase as described previously (Cheng et al., 2016), and 2X10⁵ luciferase-expressing B-ALL-*luc* cells were used per recipient mouse unless otherwise specified. All recipient animals were examined for tumor burden twice a week from the time of challenge with B-ALL *luc* injection until 70 days post-transplant, using bioluminescence imaging with the IVIS 50 and IVIS 200 imaging systems (Xenogen) as previously described (Contag and Bachmann, 2002). Each mouse was injected with 10 μ g/g body weight of luciferin and imaged for 1

minute. The bioluminescence data were analyzed and quantified with Living Image Software (Xenogen) and Igor Pro (Wave Metrics, Lake Oswego, OR). Recipient animals were evaluated for clinical score 2-3 times per week by a scoring system that sums changes in 6 clinical parameters: (1) weight loss, (2) posture, (3) activity, (4) fur texture, (5) diarrhea and (6) skin integrity (Cooke et al., 1996). Animals which lost $\geq 30\%$ of their initial body weight were euthanized.

Cytokine production assays: Animals were lethally irradiated and transplanted with donor T cells as described above. On Day 7 post-transplantation, serum was isolated from recipient mice to examine cytokines in circulation. Serum was examined for IL-33, IL-1 α , IFN- γ , TNF- α and IL-17A by multiplex cytokine assays (Biolegend LEGENDplex). For restimulation, splenocytes were processed to obtain single cells, and T cells were stimulated with anti-CD3 and anti-CD28 for 6 hours in the presence of brefeldin A (10 μ M). After 6 hours, stimulated cells were stained for surface markers and stained intracellularly for cytokines (IFN- γ and TNF- α). As a control, T cells from the same spleen were stimulated with PMA and ionomycin in the presence of brefeldin A.

Proliferation Assays: For detection of BrdU, transplanted mice (as described above) were given BrdU with an initial bolus of BrdU (2 mg per 200 μ l intraperitoneally) and drinking water containing BrdU (1 mg/ml) for 2 days. BrdU incorporation was performed using a BrDU kit (Invitrogen) according to the manufacturer's instructions.

Cytotoxicity assays: For cytotoxicity assays, luciferase-expressing A20 and B-ALL cells (both allogenic to BALB/c) were seeded in 96-well flat bottom plates at a concentration of 3×10^5 cells/ml. D-firefly luciferin potassium salt (75 μ g/ml; Caliper Hopkinton, MA) was added to each well and bioluminescence was measured with the IVIS 50 Imaging System. Subsequently, ex vivo effector cells

(MACS-sorted or FACS-sorted CD8⁺ T cells from bone marrow-transplanted mice) were added at 40:1, 20:1, and 10:1 effector-to-target (E:T) ratios and incubated at 37°C for 4 hours. Bioluminescence in relative luciferase units (RLU) was then measured for 1 minute. Cells treated with 1% Nonidet P-40 were used as a measure of maximal killing. Target cells incubated without effector cells were used to measure spontaneous death. Triplicate wells were averaged and percent lysis was calculated from the data using the following equation: % specific lysis = 100 × (spontaneous death RLU – test RLU)/(spontaneous death RLU – maximal killing RLU)(Karimi et al., 2014).

Tissue Imaging: Allo-HSCT was performed with 10X10⁶ WT T cell-depleted BM cells and 1X10⁶ FACS-sorted CD8⁺ or 1X10⁶ FACS-sorted CD4⁺ T cells (from B6-luc or SLP76Y145FKI *luc* mice) and bioluminescence imaging of tissues was performed as previously described (Beilhack et al., 2005). Briefly, 5 minutes after injection with luciferin (10 µg/g body weight), selected tissues were prepared and imaged for 5 minutes. Imaging data were analyzed and quantified with Living Image Software (Xenogen) and Igor Pro (Wave Metrics, Lake Oswego, OR).

Migration assays: Lethally irradiated BALB/c mice were injected intravenously with 10X10⁶ WT T_{CD}BM cells from B6.PL-*Thy1^a*/CyJ mice, along with FACS-sorted CD8⁺ or CD4⁺ T cells from B6.SJL (Ly5 CD45.1) and SLP76Y145FKI (C57B16 background CD45.2) mice, mixed at a 1:1 (WT: SLP76Y145FKI) ratio. Seven days post-transplantation, the mice were sacrificed and lymphocytes from the liver, small intestine, spleen, and skin-draining lymph nodes were isolated. Livers were perfused with PBS, dissociated, and filtered with a 70µm filter. The small intestines were washed in media, shaken in strip buffer at 37°C for 30 minutes to remove the epithelial cells, and then washed, before digesting with collagenase D (100 mg/ml) and DNase (1mg/ml) for 30 minutes in 37°C, and followed by filtering with a 70 µm filter. Lymphocytes from the liver and intestines were further

enriched using a 40% Percoll gradient. The cells were analyzed for CD8⁺ T cells and CD4⁺ T cells and presence of H2K^b, CD45.1⁺ and CD45.2⁺ (to identify the transferred T cell populations) by flow cytometry, but we excluded any bone marrow-derived T cells (Thy1.1⁺).

Western blotting: For protein analysis, T cells were either nonstimulated, or stimulated with anti-CD3 and anti-CD28 for 24 hours overnight, **and were** lysed with freshly prepared lysis buffer (RIPA Buffer(Fisher Scientific cat#PI89900) + cComplete Protease Inhibitor Cocktail (Sigma-Aldrich; cat# 11697498001)) and centrifuged for 10 minutes at 14000rpm at 4°C. Protein aliquots of 70µg of protein were loaded on a 12-18% denaturing polyacrylamide gel and transferred to nitrocellulose membranes for immunoblot analysis using antibodies specific to proteins of interest.

qPCR assay: Post-transplanted donor CD8⁺ and CD4⁺ T cells from C57Bl/6 mice (MHC haplotype b) were FACS sorted from recipient mice on H2K^b markers, and total RNA was isolated from T cells using the RNeasy kit from Qiagen (Germantown, MD). cDNA was made from total RNA using a cDNA synthesis kit (Invitrogen). qPCR assay was performed with a premade customized plate (CXCr3, CX3r1, CXCr1, CCR12, s1pR1, CrTAM, CXCR6, CCR9, CXCR5, CXCr4) (Fisher Scientific, Hampton, NH).

SLP76pTYR Peptide: To generate a molecule that specifically inhibits the interaction between pY145 of SLP76 and the SH2 domain of ITK, we designed a peptide based on the amino acid sequence of SLP76 from N132 to A155, which contains a phosphorylated tyrosine residue at Y145 (**Fig. 5**). To ensure that our peptide easily enters cells and that its cellular localization can be monitored, we incorporated a C-terminal TAT peptide (GRKKRRQRRRPQ) and an N-terminal fluorescent FITC dye, respectively, and named it SLP76pTYR peptide (**Fig. 5**). Both SLP76pTYR peptide (FITC Dye - ¹³²NEEEEAPVEDDADpYEPPPSNDEEA¹⁵⁵-TAT) and non-specific control peptide (FITC Dye-

IIMTTTTNKKSSRRVVVAAAADD-TAT) were synthesized by Genscript Inc (Piscataway, NJ). These peptides were initially dissolved in 3% ammonia water to a final concentration of 10 $\mu\text{g}/\mu\text{L}$ and then further diluted into PBS to a final concentration of 0.1 $\mu\text{g}/\mu\text{L}$. Fresh splenocytes were isolated from WT mice, and T cells were generated from splenocytes as previously described (Baker et al., 2001). Briefly, T cells were isolated from splenocytes using MACS beads (Miltenyi Biotec), then cultured in complete RPMI media (3×10^6 cells/mL) and plated on anti-CD3 (2.5 mg/ml; Biolegend; cat#100202) and anti-CD28 (2.5 mg/ml; Biolegend; cat#102116) antibody-coated tissue culture plates until otherwise specified. T cells were incubated with SLP76pTYR, control peptide or vehicle alone at different concentrations ranging from 100 ng/ml to 1 $\mu\text{g}/\text{ml}$ in the presence of 4 $\mu\text{g}/\text{ml}$ of protamine sulfate. Protamine sulfate significantly increased peptide delivery into primary cells. Within 60 minutes, we observed that peptides were inside the cells. Cells were cultured for 5 minutes prior to investigating signaling changes. Cells were examined for the presence of FITC by microscopy using a Leica DMI8 microscope equipped with an infinity total internal reflection fluorescence (TIRF) and DIC modules, a Lumencor SOLA SE II light box, a 150 mW 488 (GFP) laser and filter cube, a 100x/1.47 NA objective, and an Andor iXon Life 897 EMCCD camera. FITC expression was confirmed by flow cytometry as well. Cells were lysed and used in Western blots.

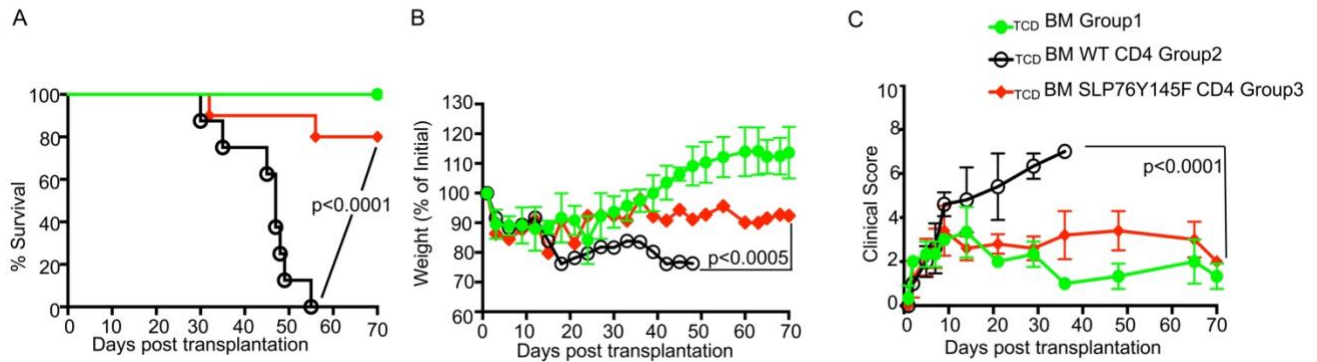
Human Samples: According to our IRB protocol (1140566-4), blood samples were obtained by vein puncture, and T cells were isolated from peripheral blood mononuclear cells (PBMC) of regular healthy donors as previously described(56). T cells were isolated from patient and healthy donor samples by Ficoll-Hypaque density centrifugation. The final product was resuspended at 3×10^6 cells/ml in media and stimulated with OKT-3/anti-CD3 (2.5 mg/ml; Ortho Bio-Tech) and anti-human CD28 (2.5 mg/ml; Biolegend; cat#302902) presence of 4 $\mu\text{g}/\text{ml}$ of protamine sulfate and 1 $\mu\text{g}/\text{ml}$ SLP76pTYR or vehicle for five minutes. T cell lysates were used in western blot analysis.

Transducing primary T cells with SLP76pTYR: We generated viruses that specifically express SLP76pTYR; the sequences encoding SLP76pTYR we cloned as a fusion protein with pCherry ordered through Integrated DNA Technology (IDT). The insert was cloned into a pQCX-I-X retroviral vector between MLU1 and Xho1 restriction sites, and the insert was confirmed by digestion and sequencing. To generate retroviral supernatants, Phoenix packaging cells were plated in 60 cm² dishes and transfected with 20 µg of the vector using Lipofectamine 2000 reagent (Invitrogen, Carlsbad, CA), according to the manufacturer's protocol. The medium was changed after 8–12 hours, and viral supernatants were harvested after 24–36 hours. Concentrated viral supernatants were re-suspended in MDM media (Invitrogen) and used to transduce primary T cells in the presence of protamine sulfate (4µg/ml) to enhance transduction efficiency. T cells were transduced with viruses containing either SLP76pTYR-pCherry or empty plasmid for 24 hours and then injected into mice.

Statistics. All numerical data are reported as means with standard deviation. Data were analyzed for significance with GraphPad Prism. Differences were determined using one-way or two-way ANOVA and Tukey's multiple comparisons tests, or with a student's t-test when necessary. *P*-values less than or equal to 0.05 are considered significant. According to power analyses, all transplant experiments were done with N=5 mice per group and repeated at least twice. Mice were sex-matched and age-matched as closely as possible.

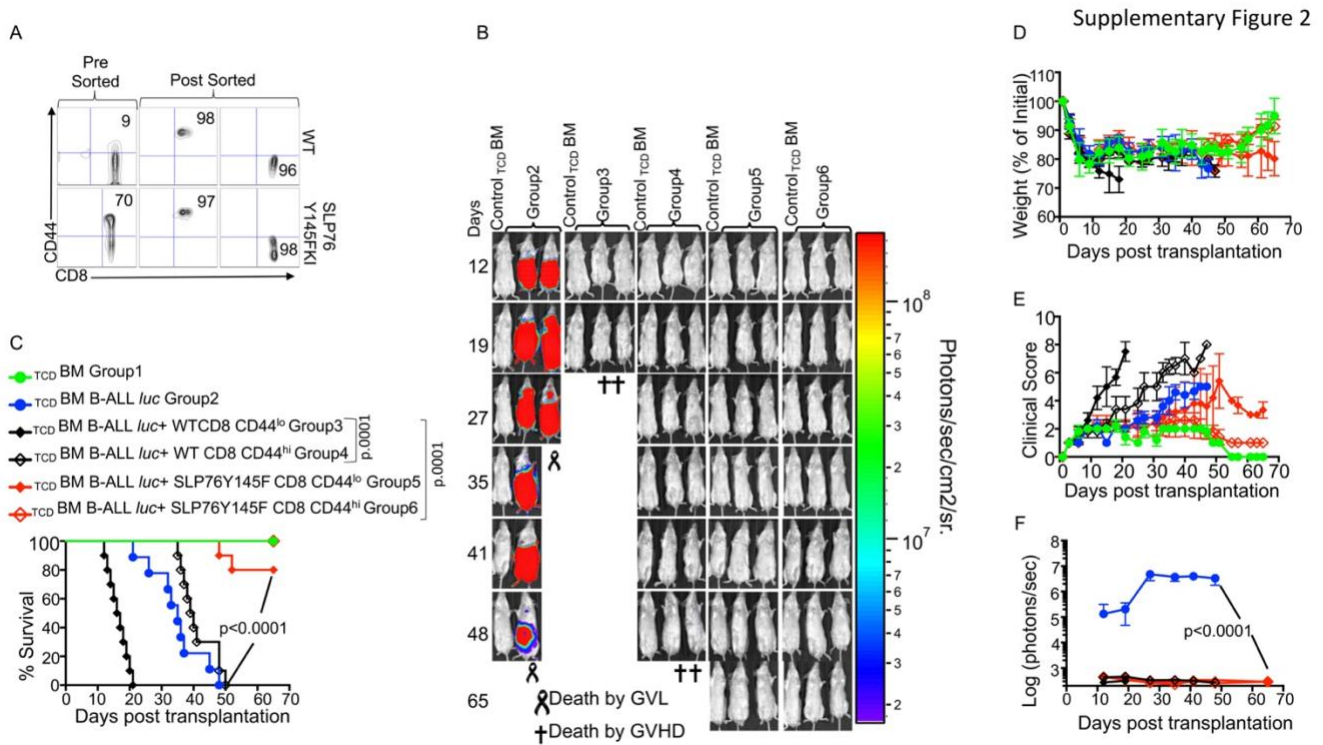
Supplementary Figure Legends

Supplementary Figure 1



Supplementary Figure 1. SLP76 Y145FKI CD4⁺ T cells exhibit attenuated induction of GVHD compared to WT T cells, Related to Figure 1.

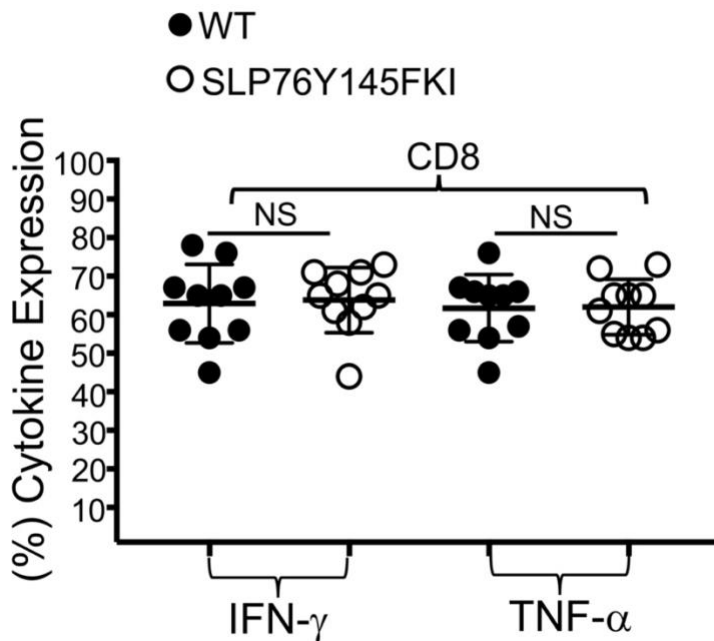
10×10^6 T cell-depleted bone marrow cells and 1×10^6 purified WT or SLP76 Y145FKI CD4⁺ T cells were transplanted into irradiated BALB/c mice. (A) The mice were monitored for survival, (B) changes in body weight, and (C) clinical score for 70 days post BMT. For weight changes and clinical score, one representative of 2 independent experiments is shown ($n = 3$ mice/group for BM alone; $n = 5$ experimental mice/group for all three groups). The p values are presented. Two-way ANOVA and Student's t -test were used for statistical analysis.



Supplementary Figure 2. The innate memory phenotype of CD8⁺ T cells does not separate GVHD and GVL effects, Related to Figure 1. (A) Purified T cells from WT and SLP76Y145FKI mice were examined for expression of CD44 pre- and post-sort. (B) All recipient BALB/c mice were lethally irradiated and divided into six different groups. Group one was transplanted with 10×10^6 TCD_{BM}. Group 2 was transplanted with 10×10^6 TCD_{BM} and 1×10^5 B-ALL-*luc*. Group 3 was transplanted with 10×10^6 TCD_{BM} along with 1×10^6 purified WT CD8⁺ CD44^{lo} T cells and 1×10^5 B-ALL-*luc*. Group 4 was transplanted with 10×10^6 TCD_{BM} along with 1×10^6 purified WT CD8⁺ CD44^{hi} T cells, and 1×10^5 B-ALL-*luc*. Group 5 was transplanted 10×10^6 TCD_{BM} along with 1×10^6 purified SLP76Y145FKI CD8⁺ CD44^{lo} T cells and 1×10^5 B-ALL-*luc*. Group 6 was transplanted with 10×10^6 TCD_{BM} and 1×10^6 purified SLP76Y145FKI CD8⁺ CD44^{hi} T cells and 1×10^5 B-ALL-*luc*. These mice were monitored for tumor growth using the IVIS 50 system. (C) The mice were monitored for survival, (D) changes in body weight, and (E) animal clinical score for 65 days post BMT. For body weight changes and clinical score, one representative of 2 independent experiments is shown (n = 3

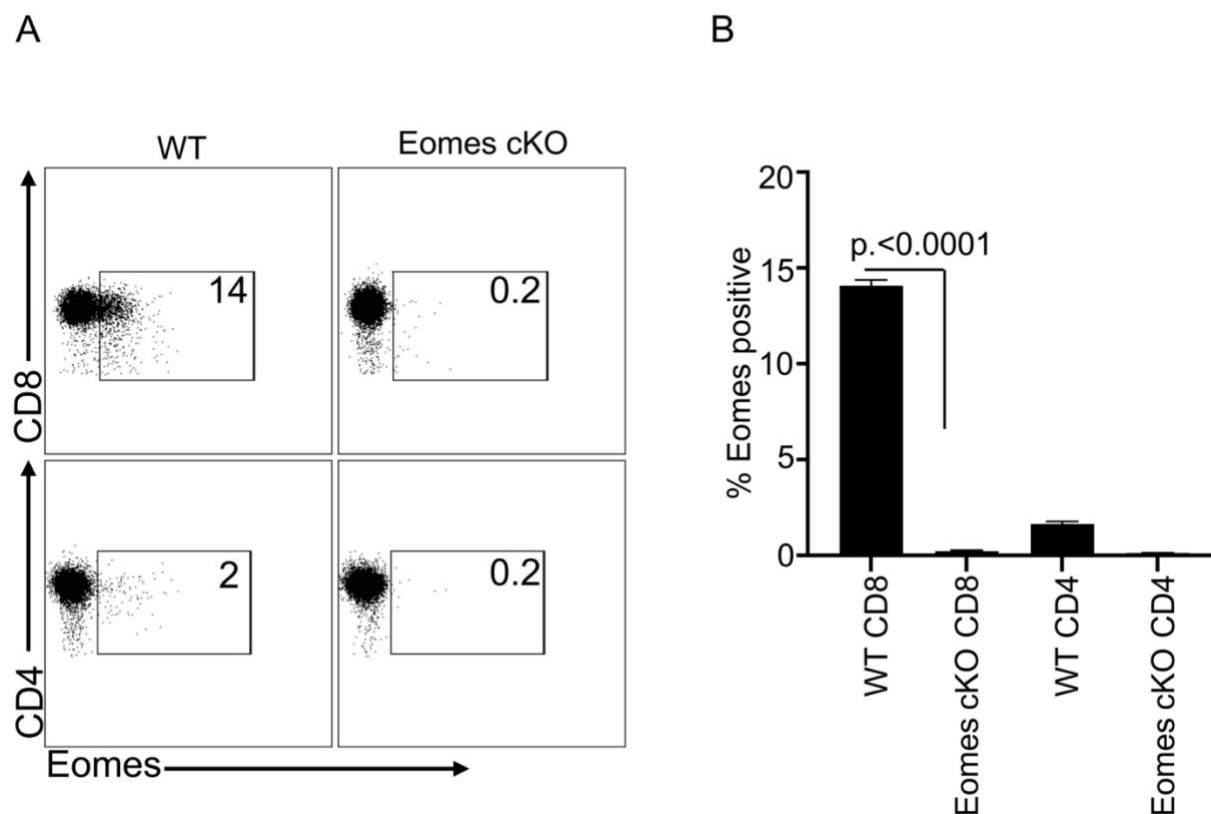
mice/group for BM alone; n = 5 experimental mice/group for all other groups. (F) Quantitated luciferase bioluminescence of luciferase-expressing B-ALL cells. Statistical analysis for survival and the clinical score was performed using the log-rank test and two-way ANOVA, respectively. *P* values are presented with each figure. *Note: Controls are naïve for tumor, but transplanted with 10X10⁶ T cell depleted bone marrow alone (T_{CD}BM) and used as a negative control for BLI.*

Supplementary Figure 3



Supplementary Figure 3. SLP76Y145FKI T cells are capable of cytokine production, Related to Figure 2. Purified T cells from WT and SLP76Y145FKI C57Bl/6 mice were transplanted into irradiated BALB/c mice (MHC haplotype d) as recipients. On day 7, donor T cells were gated for expression of H-2K^b, CD45.2, and CD45.1, and analyzed for intracellular expression of IFN- γ and TNF- α following *ex vivo* stimulation with PMA/ionomycin. Data from several experiments were combined, and statistical analysis performed using two-way ANOVA and Student's *t*-test, with *p* values presented.

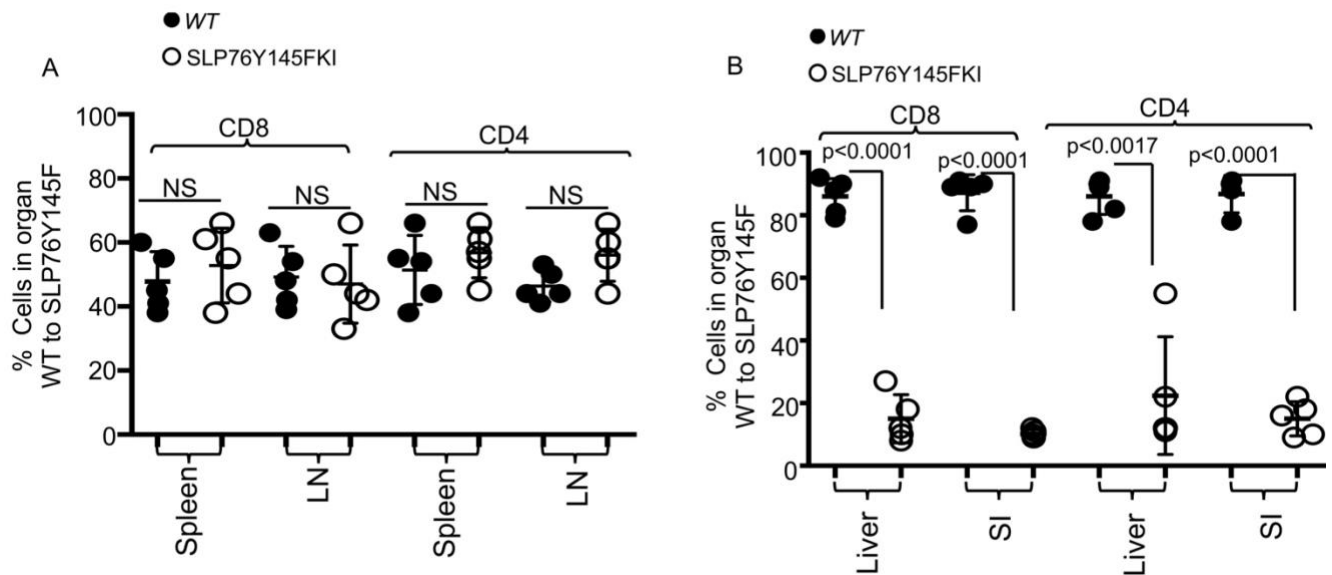
Supplementary Figure 4



Supplementary Figure 4. Eomes deletion on CD8⁺ and CD4⁺ T cells, Related to Figure 3. (A)

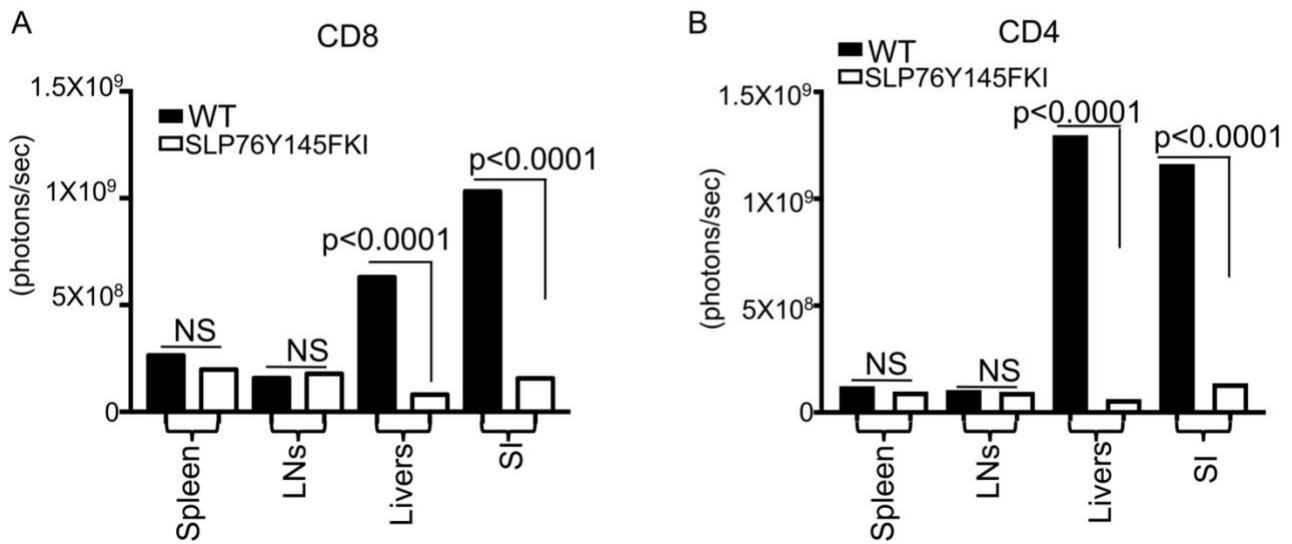
Purified donor CD8⁺ and CD4⁺ T cells from either WT or WT Eomes-deficient (Eomes cKO) mice on a C57Bl/6 background were examined for Eomes expression. (B) Quantitative analysis from flow cytometry data of several experiments. For statistical analysis we used two-way ANOVA and student's *t* test, *p* values are presented.

Supplementary Figure 5

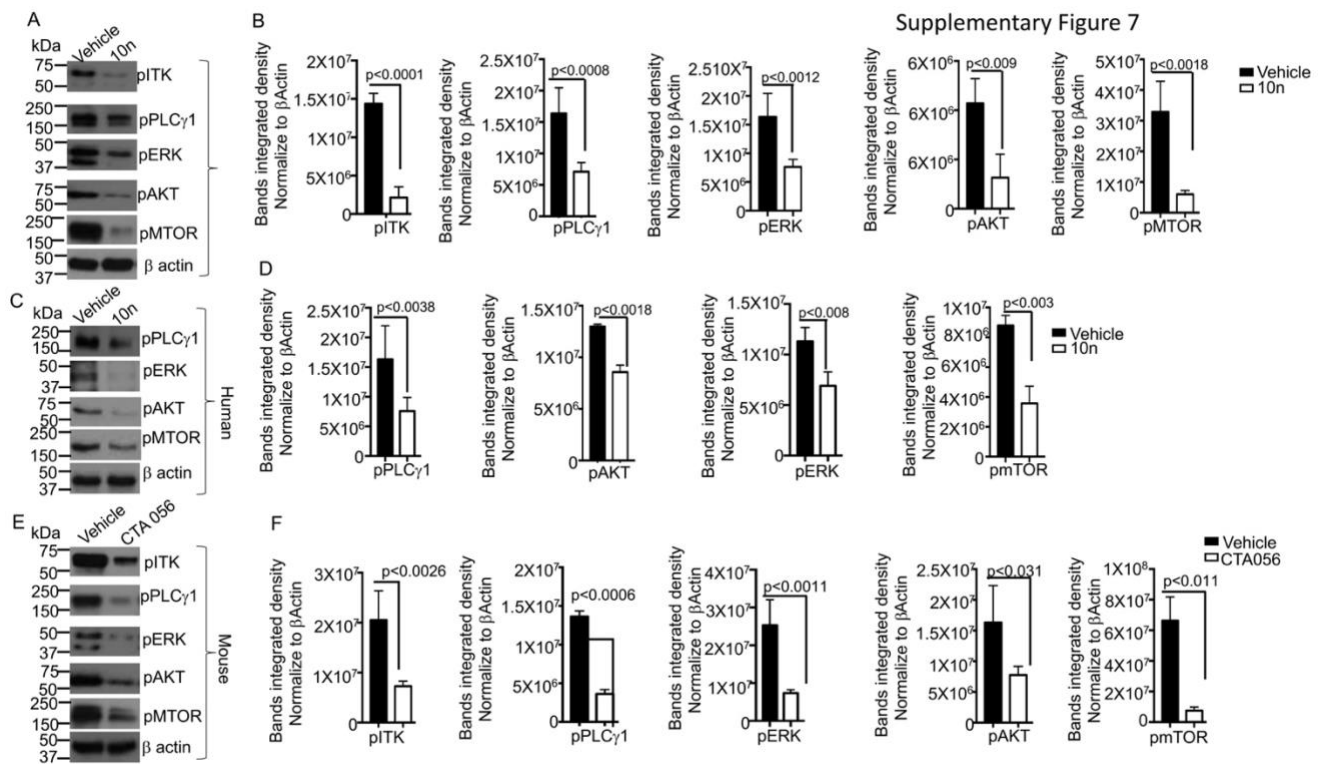


Supplementary Figure 5. Quantitative analysis of donor T cells in secondary lymphoid organs and GVHD target organs, Related to Figure 4. (A) Quantitative analysis from flow cytometry data. CD8⁺ and CD4⁺ T cells from WT and SLP76Y145FKI C57Bl/6 mice were transplanted into BALB/c mice (MHC haplotype d) as recipients. In several experiments, donor CD4⁺ and CD8⁺ T cells were analyzed for migration in the secondary lymphoid organs spleens and lymph nodes. **(B)** Quantitative analysis from flow cytometry data. In several experiments donor CD4⁺ and CD8⁺ T cells were analyzed for the presence of donor T cells in GVHD target organs, liver and small intestine. For statistical analysis we used two-way ANOVA and student's *t* test, *p* values are presented.

Supplementary Figure 6

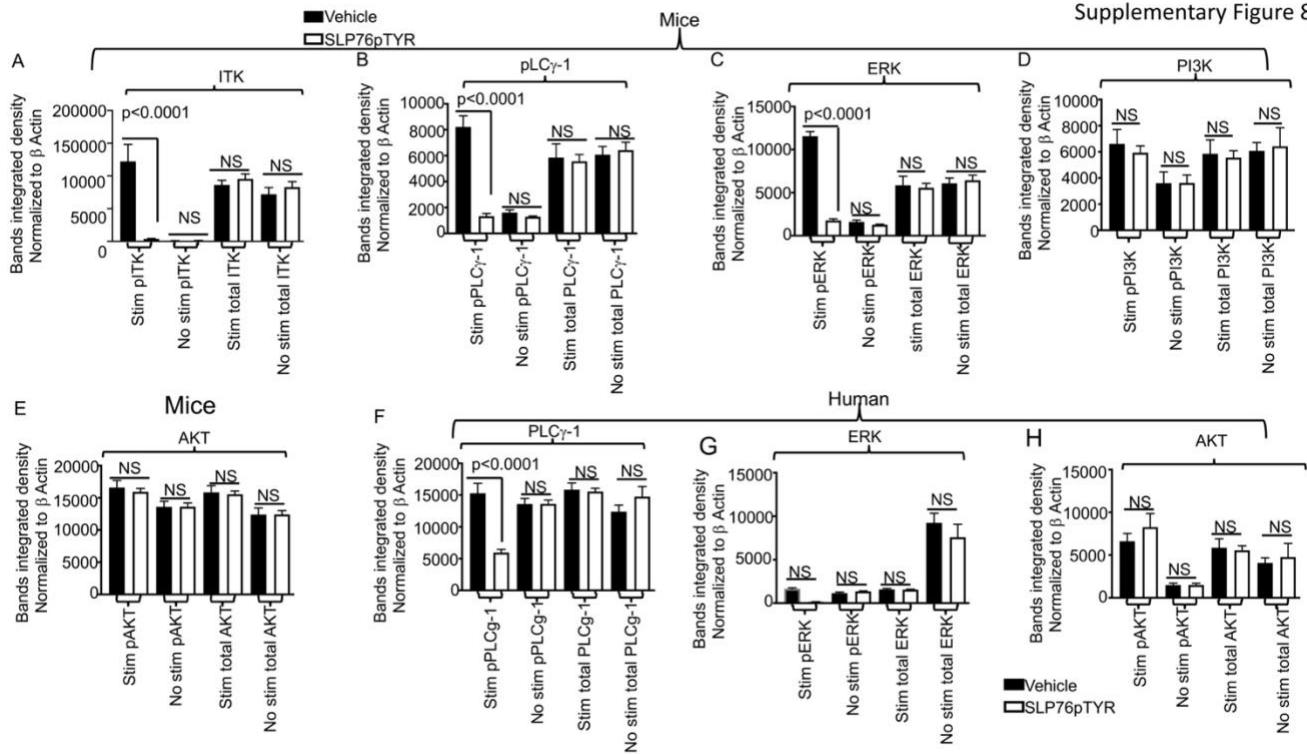


Supplementary Figure 6. Quantitative analysis of tissue bioluminescence imaging (BLI), Related to Figure 4. For tissue imaging experiments, allo-HSCT was performed with 10×10^6 WT $T_{CD}BM$ cells and 1×10^6 FACS-sorted $CD8^+$ T cells (A) or $CD4^+$ T cells (B) (from B6-luc or SLP76Y145FKI *luc* mice) and bioluminescence imaging of tissues was performed as previously described (Mammadli et al., 2020). Briefly, 5 minutes after injection with D-luciferin ($10 \mu\text{g/g}$ body weight), selected tissues were prepared and imaged for 1 minute. Imaging data were analyzed and quantified with Living Image Software (Xenogen) and Igor Pro (Wave Metrics, Lake Oswego, OR)



Supplementary Figure 7. ITK inhibitors 10n and CTA056 are not specific for ITK, Related to

Figure 5. (A) WT mouse T cells were cultured with either 10n or vehicle, then lysed post-incubation, and lysates were western blotted for pITK (size 50-75kDa), pPLC γ 1 (size ~155kDa), pERK (size ~42kDa), pAKT (size ~60kDa), and pmTOR (size 240kDa). **(B)** Western blots from three experiments were quantitated and normalized to actin. **(C)** T cells from primary human PBMCs were isolated and cultured with commercially available 10n or vehicle and western blotted for pPLC γ 1, pERK, pAKT, and pmTOR. **(D)** Western blots from three experiments were quantitated and normalized to actin. **(E)** Mouse T cells were cultured with either CTA056 or vehicle, the cells were lysed post-incubation, and lysates were western blotted for pITK, pPLC γ 1, pAKT, pmTOR, and pERK. **(F)** Western blots from three experiments were quantitated and normalized to β -Actin. Two-way ANOVA and Student's *t*-test were used for statistical analysis.



Supplementary Figure 8. Quantitative analysis of SLP76:ITK signaling protein expression in cells treated with peptide SLP76pTYR, Related to Figure 6. (A-E) Quantitative analysis of cell lysates were obtained from mouse T cells stimulated with anti-CD3 and anti-CD28 in the presence of SLP76pTYR, or vehicle alone. Lysate from stimulated cells or non-stimulated cells were examined for phosphorylated ITK, total ITK, phosphorylated PLC γ 1, total PLC γ 1, phosphorylated ERK, total ERK, phosphorylated PI3K, total PI3K, phosphorylated AKT, and total AKT. n=3 and one representative experiment is shown. **(A-E)** Quantitative analysis of cell lysates from human T cells, non-stimulated or stimulated with OKT3 for 5min in the presence of SLP76pTYR or vehicle alone, were examined for phosphorylated pPLC γ 1 and total PLC γ 1 on stimulated and non-stimulated T cells. Cell lysate from stimulated and non-stimulated cells were examine for pERK and total ERK. Lysates from stimulated and non-stimulated were also examined for phosphorylation and total AKT. n=3 and one representative experiment is shown.

Reference

- BAKER, J., VERNERIS, M. R., ITO, M., SHIZURU, J. A. & NEGRIN, R. S. 2001. Expansion of cytolytic CD8(+) natural killer T cells with limited capacity for graft-versus-host disease induction due to interferon gamma production. *Blood*, 97, 2923-31.
- BEILHACK, A., SCHULZ, S., BAKER, J., BEILHACK, G. F., WIELAND, C. B., HERMAN, E. I., BAKER, E. M., CAO, Y. A., CONTAG, C. H. & NEGRIN, R. S. 2005. In vivo analyses of early events in acute graft-versus-host disease reveal sequential infiltration of T-cell subsets. *Blood*, 106, 1113-22.
- CHENG, Y., CHIKWAVA, K., WU, C., ZHANG, H., BHAGAT, A., PEI, D., CHOI, J. K. & TONG, W. 2016. LNK/SH2B3 regulates IL-7 receptor signaling in normal and malignant B-progenitors. *J Clin Invest*, 126, 1267-81.
- CONTAG, C. H. & BACHMANN, M. H. 2002. Advances in in vivo bioluminescence imaging of gene expression. *Annu Rev Biomed Eng*, 4, 235-60.
- COOKE, K. R., KOBZIK, L., MARTIN, T. R., BREWER, J., DELMONTE, J., JR., CRAWFORD, J. M. & FERRARA, J. L. 1996. An experimental model of idiopathic pneumonia syndrome after bone marrow transplantation: I. The roles of minor H antigens and endotoxin. *Blood*, 88, 3230-9.
- EDINGER, M., HOFFMANN, P., ERMANN, J., DRAGO, K., FATHMAN, C. G., STROBER, S. & NEGRIN, R. S. 2003. CD4+CD25+ regulatory T cells preserve graft-versus-tumor activity while inhibiting graft-versus-host disease after bone marrow transplantation. *Nat Med*, 9, 1144-50.
- JORDAN, M. S., SMITH, J. E., BURNS, J. C., AUSTIN, J. E., NICHOLS, K. E., ASCHENBRENNER, A. C. & KORETZKY, G. A. 2008. Complementation in trans of altered thymocyte development in mice expressing mutant forms of the adaptor molecule SLP76. *Immunity*, 28, 359-69.
- KARIMI, M. A., LEE, E., BACHMANN, M. H., SALICIONI, A. M., BEHRENS, E. M., KAMBAYASHI, T. & BALDWIN, C. L. 2014. Measuring cytotoxicity by bioluminescence imaging outperforms the standard chromium-51 release assay. *PLoS One*, 9, e89357.
- MAMMADLI, M., HUANG, W., HARRIS, R., SULTANA, A., CHENG, Y., TONG, W., PU, J., GENTILE, T., DSOUZA, S., YANG, Q., BAH, A., AUGUST, A. & KARIMI, M. 2020. Targeting Interleukin-2-Inducible T-Cell Kinase (ITK) Differentiates GVL and GVHD in Allo-HSCT. *Front Immunol*, 11, 593863.